ECCOMAS Congress 2016
VII European Congress on Computational Methods in Applied Sciences and Engineering
M. Papadrakakis, V. Papadopoulos, G. Stefanou, V. Plevris (eds.)
Crete Island, Greece, 5–10 June 2016

STRUCTURE-PRESERVING OPTIMAL CONTROL OF DISCRETE MECHANICAL SYSTEMS

Peter Betsch[1] **and Christian Becker**[1]

[1]Institute of Mechanics
Karlsruhe Institute of Technology (KIT)
Otto-Ammann-Platz 9
76131 Karlsruhe, Germany
{peter.betsch, christian.becker}@kit.edu

Keywords: Structure-Preserving Methods; Optimal Control; Noether's Theorem; Rotational symmetry; Generalized Momentum Maps

Abstract. *In this paper a structure-preserving direct method for the optimal control of mechanical systems is developed. The new method accommodates a large class of one-step integrators for the underlying state equations. The state equations under consideration govern the motion of affine Hamiltonian control systems. If the optimal control problem has symmetry, associated generalized momentum maps are conserved along an optimal path. This is in accordance with an extension of Noether's theorem to the realm of optimal control problems. In the present work we focus on optimal control problems with rotational symmetries. The newly proposed direct approach is capable of exactly conserving generalized momentum maps associated with rotational symmetries of the optimal control problem. This is true for a variety of one-step integrators used for the discretization of the state equations. Examples are the one-step theta method, a partitioned variant of the theta method, and energy-momentum consistent integrators. Numerical investigations confirm the theoretical findings.*

1 INTRODUCTION

The present work deals with the design of structure-preserving numerical methods for the solution of optimal control problems in mechanics. Although there exist many alternative numerical methods for the solution of optimal control problems (see, for example, the books by Agrawal & Fabien [1], Betts [4], Biegler [5] and Gerdts [14], and the survey articles by Binder et al. [6] und Diehl et al. [11]), little attention has been paid to structure-preservation on the level of the optimal control problem.

It is well-known that the Hamiltonian of autonomous optimal control problems is conserved along an optimal path (see, for example, Little & Pinch [23]). In addition to that, the optimal control problem may inherit symmetries from the underlying control system. Typically, in the context of mechanical control systems rotational symmetries are of paramount importance. Due to a generalization of Noether's theorem to optimal control (see Djukić [12] and Torres [28, 29]), symmetries of the optimal control problem lead to associated generalized momentum maps that are conserved along an optimal path. In the case of mechanical systems these symmetries have been explored to reduce the dimension of the optimal control problem (see Grizzle & Marcus [16] and van der Schaft [30]). However, to the best of our knowledge, symmetries and associated momentum maps have not been taken into account in the development of structure-preserving numerical methods for optimal control.

In contrast to that, structure-preserving numerical integrators originally developed in the framework of Hamiltonian systems with symmetry have been recently employed in the optimal control of mechanical systems. These integrators are capable of conserving important mechanical quantities in the forward dynamics of mechanical systems. In particular, energy-momentum integrators yield algorithmic conservation of energy and angular momentum in the case of Hamiltonian systems with rotational symmetry. Similarly, symplectic-momentum integrators are capable of conserving angular momentum and preserve the symplectic transformation property in phase space.

Structure-preserving numerical integrators can be directly used in optimal control problems by applying the direct transcription approach. For example, energy-momentum integrators have been used in the solution of optimal control problems by Bottasso & Croce [9], Betsch et al. [3] and Koch & Leyendecker [21]. Similarly, symplectic-momentum integrators have been applied in the framework of the direct approach to optimal control problems by Leyendecker et al. [22], Ober-Blöbaum et al. [26] and Bloch et al. [8].

In the present work we focus on mechanical optimal control problems with rotational symmetries. We propose a new direct approach to the design of structure-preserving schemes that are capable of conserving generalized momentum maps associated with rotational symmetries on the level of the optimal control problem. The newly proposed method accommodates a whole family of one-step integrators for the underlying state equations. Among those one-step integrators are the symplectic Euler methods, the implicit mid-point rule and 2nd-order accurate energy-momentum schemes. By design, the proposed method exactly conserves the generalized momentum maps associated with rotational symmetries of the optimal control problem, independent of the underlying integrator and the number of time steps used to resolve the time interval of interest.

An outline of the rest of the paper is as follows. In Section 2 we summarize the equations governing both the mechanical control systems and the optimal control problems under investigation. In particular, conditions for the presence of rotational symmetries are provided, the

form of the associated generalized momentum maps is addressed, and a proof of the Noether-type conservation law on the level of the optimal control problem is given. Section 3 contains the newly proposed structure-preserving method. The generation of specific optimal control schemes based on the choice of specific one-step integrators for the state equations is presented in Section 4. These schemes are further investigated in Section 5 with the numerical example of a nonlinear spring pendulum. Eventually, conclusions are drawn in Section 6.

2 GOVERNING EQUATIONS

In the present work we consider finite-dimensional mechanical control systems whose motion is governed by state equations of the form

$$\dot{\boldsymbol{x}} = \boldsymbol{f}(\boldsymbol{x}, \boldsymbol{u}) \tag{1}$$

Here, the vector of state coordinates $\boldsymbol{x} = (\boldsymbol{q}, \boldsymbol{p}) \in \mathcal{P} \equiv \mathbb{R}^{2n}$ contains the configuration coordinates $\boldsymbol{q} \in \mathcal{Q} \equiv \mathbb{R}^n$ and the momenta $\boldsymbol{p} \in \mathbb{R}^n$. Accordingly, the configuration space $\mathcal{Q}$ is assumed to be linear and the state space $\mathcal{P}$ coincides with the canonical phase space ($\mathcal{P} = T^*\mathcal{Q}$). The momentum vector can be written in the form $\boldsymbol{p} = \boldsymbol{M}\dot{\boldsymbol{q}}$, where $\boldsymbol{M} \in \mathbb{R}^{n\times n}$ is a non-singular mass matrix and $\dot{\boldsymbol{q}} = \frac{d}{dt}\boldsymbol{q} \in \mathbb{R}^n (= T_q\mathcal{Q})$ denotes the velocity vector. On the right-hand side of (1), $\boldsymbol{f} : \mathcal{P} \times \mathcal{U} \mapsto \mathbb{R}^{2n}$ is a continuously differentiable function and $\boldsymbol{u} \in \mathcal{U} \subset \mathbb{R}^m$ are the controls. In the present work we restrict ourselves to **affine Hamiltonian control systems** (see, for example, Bloch [7]), so that a more detailed form of the state equations (1) is given by

$$\begin{aligned} \dot{\boldsymbol{q}} &= \partial_{\boldsymbol{p}}\mathcal{H}(\boldsymbol{q}, \boldsymbol{p}) \\ \dot{\boldsymbol{p}} &= -\partial_{\boldsymbol{q}}\mathcal{H}(\boldsymbol{q}, \boldsymbol{p}) + \boldsymbol{B}(\boldsymbol{q})\boldsymbol{u} \end{aligned} \tag{2}$$

Here, $\mathcal{H} : \mathcal{P} \mapsto \mathbb{R}$ is the Hamiltonian of the mechanical system and $\boldsymbol{B}(\boldsymbol{q}) \in \mathbb{R}^{n\times m}$ is a control distribution matrix. In the uncontrolled case (i.e. if $\boldsymbol{u} = \boldsymbol{0}$), the Hamiltonian control system (2) reduces to a standard Hamiltonian system which we call the **underlying Hamiltonian system**. In the sequel we focus on natural mechanical systems with **separable** Hamiltonians of the form

$$\mathcal{H}(\boldsymbol{q}, \boldsymbol{p}) = \frac{1}{2}\boldsymbol{p} \cdot \boldsymbol{M}^{-1}\boldsymbol{p} + \mathcal{V}(\boldsymbol{q}) \tag{3}$$

where $\mathcal{V} : \mathcal{Q} \mapsto \mathbb{R}$ is the potential energy. In the following it often proofs convenient to use 'nodal' configuration vectors $\boldsymbol{q}_I \in \mathbb{R}^3$ and associated nodal momentum vectors $\boldsymbol{p}^I \in \mathbb{R}^3$, so that the state coordinates of the system are comprised of partitioned configuration and momentum vectors

$$\begin{aligned} \boldsymbol{q} &= \left(\boldsymbol{q}_1, \boldsymbol{q}_2, \ldots, \boldsymbol{q}_{n_n}\right) \in \mathbb{R}^{3n_n} \\ \boldsymbol{p} &= \left(\boldsymbol{p}^1, \boldsymbol{p}^2, \ldots, \boldsymbol{p}^{n_n}\right) \in \mathbb{R}^{3n_n} \end{aligned} \tag{4}$$

where n_n denotes the number of nodes. To summarize, in the present work we focus on mechanical control systems whose state equations are given by

$$\begin{aligned} \dot{\boldsymbol{q}} &= \boldsymbol{f}^q(\boldsymbol{p}) = \boldsymbol{M}^{-1}\boldsymbol{p} \\ \dot{\boldsymbol{p}} &= \boldsymbol{f}_p(\boldsymbol{q}, \boldsymbol{u}) \end{aligned} \quad \text{or} \quad \begin{aligned} \dot{\boldsymbol{q}}_I &= \boldsymbol{f}^q_I(\boldsymbol{p}) = (M^{-1})_{IJ}\boldsymbol{p}^J \\ \dot{\boldsymbol{p}}^I &= \boldsymbol{f}^I_p(\boldsymbol{q}, \boldsymbol{u}) = -\partial_{\boldsymbol{q}_I}\mathcal{V}(\boldsymbol{q}) + \boldsymbol{f}^I_{\text{ext}}(\boldsymbol{q}, \boldsymbol{u}) \end{aligned} \tag{5}$$

Note that the control forces are contained in

$$\boldsymbol{f}^I_{\text{ext}}(\boldsymbol{q}, \boldsymbol{u}) = \boldsymbol{B}^I_j(\boldsymbol{q})u^j$$

In this connection $(M^{-1})_{IJ}$ denotes the components of $\boldsymbol{M}^{-1}$ corresponding to the nodes I and J. Throughout this work the summation convention applies to repeated lower case and upper case letters. The state equations (5) govern, for example, the controlled motion of (i) n_n particles in 3-space, (ii) semi-discrete systems arising from the discretization in space of nonlinear elastodynamics, and (iii) elastic Cosserat points.

2.1 Optimal control problem

Assume that on a time interval $\mathcal{I} = [0, T]$, the mechanical system under consideration is to be steered from an initial state $\boldsymbol{x}(0) = \overline{\boldsymbol{x}}_0 \in \mathcal{P}$ to a terminal state specified by the terminal constraint $\boldsymbol{g}_T(\boldsymbol{x}(T)) = \boldsymbol{0}$, $\boldsymbol{g}_T : \mathcal{P} \mapsto \mathbb{R}^{n_T}$, $n_T \leq 2n$, such that a specific cost functional is minimized. The corresponding **optimal control problem** is given by

$$J[\boldsymbol{x}(\cdot), \boldsymbol{u}(\cdot)] = K(\boldsymbol{x}(T)) + \int_0^T L(\boldsymbol{x}(t), \boldsymbol{u}(t))dt \longrightarrow \text{min}$$

subject to

$$\begin{aligned} \dot{\boldsymbol{x}} &= \boldsymbol{f}(\boldsymbol{x}, \boldsymbol{u}) \\ \boldsymbol{x}(0) &= \overline{\boldsymbol{x}}_0 \\ \boldsymbol{0} &= \boldsymbol{g}_T(\boldsymbol{x}(T)) \\ \boldsymbol{u} &\in \mathcal{U} \end{aligned}$$

Here, $L : \mathcal{P} \times \mathcal{U} \mapsto \mathbb{R}$ denotes the density cost function and $K : \mathcal{P} \mapsto \mathbb{R}$ is the final cost function. Since we focus on structural properties of the optimal control problem, we make the simplifying assumption $\mathcal{U} \equiv \mathbb{R}^m$, that is, there are no constraints on the controls. In accordance with the Pontryagin maximum principle we introduce the Hamiltonian of the optimal control problem $H : \mathcal{P} \times \mathbb{R}^{2n} \times \mathcal{U} \mapsto \mathbb{R}$ given by

$$H(\boldsymbol{x}, \boldsymbol{\psi}, \boldsymbol{u}) = \boldsymbol{\psi} \cdot \boldsymbol{f}(\boldsymbol{x}, \boldsymbol{u}) - L(\boldsymbol{x}, \boldsymbol{u}) \tag{6}$$

Now necessary conditions for the optimality of a solution $(\boldsymbol{x}^*(t), \boldsymbol{u}^*(t))$ to the optimal control problem are given by

$$\dot{\boldsymbol{x}} = \partial_{\boldsymbol{\psi}} H(\boldsymbol{x}, \boldsymbol{\psi}, \boldsymbol{u}) = \boldsymbol{f}(\boldsymbol{x}, \boldsymbol{u}) \tag{7a}$$

$$\dot{\boldsymbol{\psi}} = -\partial_{\boldsymbol{x}} H(\boldsymbol{x}, \boldsymbol{\psi}, \boldsymbol{u}) = \partial_{\boldsymbol{x}} L(\boldsymbol{x}, \boldsymbol{u}) - \boldsymbol{\psi} \cdot \partial_{\boldsymbol{x}} \boldsymbol{f}(\boldsymbol{x}, \boldsymbol{u}) \tag{7b}$$

$$\boldsymbol{0} = \partial_{\boldsymbol{u}} H(\boldsymbol{x}, \boldsymbol{\psi}, \boldsymbol{u}) = -\partial_{\boldsymbol{u}} L(\boldsymbol{x}, \boldsymbol{u}) + \boldsymbol{\psi} \cdot \partial_{\boldsymbol{u}} \boldsymbol{f}(\boldsymbol{x}, \boldsymbol{u}) \tag{7c}$$

together with the endpoint conditions

$$\boldsymbol{x}(0) = \overline{\boldsymbol{x}}_0 \tag{8a}$$

$$\boldsymbol{0} = \boldsymbol{g}_T(\boldsymbol{x}(T)) \tag{8b}$$

$$\boldsymbol{\psi}(T) = -DK(\boldsymbol{x}(T)) - D\boldsymbol{g}_T(\boldsymbol{x}(T))^T \boldsymbol{\eta} \tag{8c}$$

Accordingly, in addition to the state equations (7a), the necessary conditions consist of the adjoint equations (7b) along with the control equations (7c). The variables $\boldsymbol{\psi} \in \mathbb{R}^{2n}$ in (7b) are termed adjoint (or costate) variables. Moreover, $\boldsymbol{\eta} \in \mathbb{R}^{n_T}$ in (8c) are Lagrange multipliers associated with the terminal constraints (8b). Note that the endpoint conditions (8) consist of

a mixed set of initial and terminal conditions. Altogether the system of differential algebraic equations (7) together with the endpoint conditions (8) constitute a two-point boundary value problem.

In analogy to the partitioning of the state coordinates the adjoint variables can be arranged in partitioned form $\boldsymbol{\psi} = (\boldsymbol{\psi}_q, \boldsymbol{\psi}^p)$. Then the adjoint equations (7b) can be written as

$$\begin{aligned} \dot{\boldsymbol{\psi}}_q &= \partial_{\boldsymbol{q}} L\big((\boldsymbol{q},\boldsymbol{p}),\boldsymbol{u}\big) - \boldsymbol{\psi}^p \cdot \partial_{\boldsymbol{q}} \boldsymbol{f}_p(\boldsymbol{q},\boldsymbol{u}) \\ \dot{\boldsymbol{\psi}}^p &= \partial_{\boldsymbol{p}} L\big((\boldsymbol{q},\boldsymbol{p}),\boldsymbol{u}\big) - \boldsymbol{\psi}_q \cdot \partial_{\boldsymbol{p}} \boldsymbol{f}^q(\boldsymbol{p}) \end{aligned} \tag{9}$$

In addition to that, the control equations (7c) can be recast in the form

$$\boldsymbol{0} = \partial_{\boldsymbol{u}} L\big((\boldsymbol{q},\boldsymbol{p}),\boldsymbol{u}\big) - \boldsymbol{\psi}^p \cdot \partial_{\boldsymbol{u}} \boldsymbol{f}_p(\boldsymbol{q},\boldsymbol{u}) \tag{10}$$

Moreover, using the partitioned form of the state and adjoint variables, the optimal control Hamiltonian (6) may also be written in the form

$$H\left((\boldsymbol{q},\boldsymbol{p}),(\boldsymbol{\psi}_q,\boldsymbol{\psi}^p),\boldsymbol{u}\right) = \boldsymbol{\psi}_q \cdot \boldsymbol{f}^q(\boldsymbol{p}) + \boldsymbol{\psi}^p \cdot \boldsymbol{f}_p(\boldsymbol{q},\boldsymbol{u}) - L((\boldsymbol{q},\boldsymbol{p}),\boldsymbol{u}) \tag{11a}$$

$$= \boldsymbol{\psi}_q^I \cdot \boldsymbol{f}_I^q(\boldsymbol{p}) + \boldsymbol{\psi}_I^p \cdot \boldsymbol{f}_p^I(\boldsymbol{q},\boldsymbol{u}) - L((\boldsymbol{q},\boldsymbol{p}),\boldsymbol{u}) \tag{11b}$$

Note that this notation is consistent with the partitioned form of the state equations (5). In (11b) nodal quantities consistent with (4) have been used. In what follows these alternative partitioned forms will be employed occasionally.

2.2 Symmetries of the optimal control problem

We focus on rotational symmetries of a mechanical system related to a one-parameter family of rotation matrices $\boldsymbol{R}^s \in \mathrm{SO}(3)$, the special orthogonal group in 3-space. In particular, we consider superposed rotations of the form

$$\begin{aligned} \boldsymbol{q}_I^s &= \boldsymbol{R}^s \boldsymbol{q}_I \\ (\boldsymbol{p}^I)^s &= \boldsymbol{R}^s \boldsymbol{p}^I \end{aligned} \tag{12}$$

for $I = 1, \ldots, n_n$, and $\boldsymbol{R}^s = \exp(s\widehat{\boldsymbol{\xi}}) \in \mathrm{SO}(3)$, where the exponential map is given by the Rodrigues formula (see, for example, [25])

$$\exp(s\widehat{\boldsymbol{\xi}}) = \boldsymbol{I} + \frac{\sin(s\|\boldsymbol{\xi}\|)}{\|\boldsymbol{\xi}\|}\widehat{\boldsymbol{\xi}} + \frac{1}{2}\left[\frac{\sin(s\|\boldsymbol{\xi}\|/2)}{\|\boldsymbol{\xi}/2\|}\right]^2 \widehat{\boldsymbol{\xi}}^2 \tag{13}$$

Here, $\widehat{\boldsymbol{\xi}} \in \mathrm{so}(3)$ is a skew-symmetric tensor with associated axial vector $\boldsymbol{\xi} \in \mathbb{R}^3$. That is, $\widehat{\boldsymbol{\xi}}\boldsymbol{a} = \boldsymbol{\xi} \times \boldsymbol{a}$ for any $\boldsymbol{a} \in \mathbb{R}^3$. In the present context $\boldsymbol{\xi}$ is a fixed non-zero vector in $\mathbb{R}^3$. It can be easily verified that $\boldsymbol{R}^s = \exp(s\widehat{\boldsymbol{\xi}})$ satisfies

$$\boldsymbol{R}^{s=0} = \boldsymbol{I} \qquad \text{and} \qquad \left.\frac{d}{ds}\right|_{s=0} \boldsymbol{R}^s = \widehat{\boldsymbol{\xi}}$$

Thus we have $\boldsymbol{q}_I^0 = \boldsymbol{q}_I$, $(\boldsymbol{p}^I)^0 = \boldsymbol{p}^I$, along with the infinitesimal generators

$$\begin{aligned} \left.\frac{d}{ds}\right|_{s=0} \boldsymbol{q}_I^s &= \boldsymbol{\xi} \times \boldsymbol{q}_I \\ \left.\frac{d}{ds}\right|_{s=0} (\boldsymbol{p}^I)^s &= \boldsymbol{\xi} \times \boldsymbol{p}^I \end{aligned} \tag{14}$$

2.2.1 Symmetry of the mechanical control system

Let a one-parameter family of maps on $\mathcal{P}$ be given by (12). The mechanical control system (5) has rotational symmetry if there exist controls $\boldsymbol{u}^s(t) \in \mathcal{U}$, where $\boldsymbol{u}^0(t) = \boldsymbol{u}(t)$, such that

$$\begin{aligned} \boldsymbol{R}^s \boldsymbol{f}_I^q(\boldsymbol{p}) &= \boldsymbol{f}_I^q(\boldsymbol{R}^s \circ \boldsymbol{p}) \\ \boldsymbol{R}^s \boldsymbol{f}_p^I(\boldsymbol{q}, \boldsymbol{u}) &= \boldsymbol{f}_p^I(\boldsymbol{R}^s \circ \boldsymbol{q}, \boldsymbol{u}^s) \end{aligned} \tag{15}$$

where the shorthand notation

$$\begin{aligned} \boldsymbol{R}^s \circ \boldsymbol{q} &= \left(\boldsymbol{R}^s \boldsymbol{q}_1, \ldots, \boldsymbol{R}^s \boldsymbol{q}_{n_n}\right) \\ \boldsymbol{R}^s \circ \boldsymbol{p} &= \left(\boldsymbol{R}^s \boldsymbol{p}^1, \ldots, \boldsymbol{R}^s \boldsymbol{p}^{n_n}\right) \end{aligned}$$

has been introduced.

2.2.2 Symmetry of the optimal control problem

The optimal control problem has symmetry if, in addition to the symmetry of the mechanical control system, (15), the density cost function is invariant under superposed rotations. That is,

$$L\left(\boldsymbol{R}^s \circ \boldsymbol{q}, \boldsymbol{R}^s \circ \boldsymbol{p}, \boldsymbol{u}^s\right) = L\left(\boldsymbol{q}, \boldsymbol{p}, \boldsymbol{u}\right) \tag{16}$$

According to the generalization of Noether's theorem to optimal control, the symmetry of an optimal control problem implies the conservation of a generalized momentum map. In the present case, the rotational symmetry of the optimal control problem under consideration is associated with a generalized momentum map of the form

$$J_\xi(\boldsymbol{q}, \boldsymbol{p}, \boldsymbol{\psi}_q, \boldsymbol{\psi}^p) = \boldsymbol{\xi} \cdot \left(\boldsymbol{q}_I \times \boldsymbol{\psi}_q^I + \boldsymbol{p}^I \times \boldsymbol{\psi}_I^p\right) \tag{17}$$

The generalized momentum map (65) is conserved provided that conditions (15) and (16) are satisfied. This can be shown by a direct calculation along the lines of Torres [29]. We start with the infinitesimal version of the symmetry condition (16) given by

$$\begin{aligned} \left.\frac{d}{ds}\right|_{s=0} L\left(\boldsymbol{R}^s \circ \boldsymbol{q}, \boldsymbol{R}^s \circ \boldsymbol{p}, \boldsymbol{u}^s\right) &= 0 \\ \partial_{\boldsymbol{q}_I} L(\boldsymbol{q}, \boldsymbol{p}, \boldsymbol{u}) \cdot \widehat{\boldsymbol{\xi}} \boldsymbol{q}_I + \partial_{\boldsymbol{p}^I} L(\boldsymbol{q}, \boldsymbol{p}, \boldsymbol{u}) \cdot \widehat{\boldsymbol{\xi}} \boldsymbol{p}^I + \partial_{\boldsymbol{u}} L(\boldsymbol{q}, \boldsymbol{p}, \boldsymbol{u}) \cdot \left.\frac{d}{ds}\right|_{s=0} \boldsymbol{u}^s &= 0 \end{aligned} \tag{18}$$

where use has been made of (14). Inserting from the adjoint equations (9) and the control equations (10) into the last equation yields

$$\left(\dot{\boldsymbol{\psi}}_q^I + \boldsymbol{\psi}^p \cdot \partial_{\boldsymbol{q}_I} \boldsymbol{f}_p(\boldsymbol{q}, \boldsymbol{u})\right) \cdot \widehat{\boldsymbol{\xi}} \boldsymbol{q}_I + \left(\dot{\boldsymbol{\psi}}_I^p + \boldsymbol{\psi}_q \cdot \partial_{\boldsymbol{p}^I} \boldsymbol{f}^q(\boldsymbol{p})\right) \cdot \widehat{\boldsymbol{\xi}} \boldsymbol{p}^I + \boldsymbol{\psi}^p \cdot \partial_{\boldsymbol{u}} \boldsymbol{f}_p(\boldsymbol{q}, \boldsymbol{u}) \left.\frac{d}{ds}\right|_{s=0} \boldsymbol{u}^s = 0$$

The last equation can be recast in the form

$$\dot{\boldsymbol{\psi}}_q^I \cdot \widehat{\boldsymbol{\xi}} \boldsymbol{q}_I + \dot{\boldsymbol{\psi}}_I^p \cdot \widehat{\boldsymbol{\xi}} \boldsymbol{p}^I + \boldsymbol{\psi}_q^I \cdot \partial_{\boldsymbol{p}^J} \boldsymbol{f}_I^q(\boldsymbol{p}) \widehat{\boldsymbol{\xi}} \boldsymbol{p}^J + \boldsymbol{\psi}_I^p \cdot \left(\partial_{\boldsymbol{q}_J} \boldsymbol{f}_p^I(\boldsymbol{q}, \boldsymbol{u}) \widehat{\boldsymbol{\xi}} \boldsymbol{q}_J + \partial_{\boldsymbol{u}} \boldsymbol{f}_p^I(\boldsymbol{q}, \boldsymbol{u}) \left.\frac{d}{ds}\right|_{s=0} \boldsymbol{u}^s\right) = 0$$

Performing the derivative $d/ds|_{s=0}$ of (15) and taking into account the state equations (5), we obtain

$$\begin{aligned} \partial_{\boldsymbol{p}^J} \boldsymbol{f}_I^q(\boldsymbol{p}) \widehat{\boldsymbol{\xi}} \boldsymbol{p}^J &= \widehat{\boldsymbol{\xi}} \boldsymbol{f}_I^q(\boldsymbol{p}) &&= \widehat{\boldsymbol{\xi}} \dot{\boldsymbol{q}}_I \\ \partial_{\boldsymbol{q}_J} \boldsymbol{f}_p^I(\boldsymbol{q}, \boldsymbol{u}) \widehat{\boldsymbol{\xi}} \boldsymbol{q}_J + \partial_{\boldsymbol{u}} \boldsymbol{f}_p^I(\boldsymbol{q}, \boldsymbol{u}) \left.\tfrac{d}{ds}\right|_{s=0} \boldsymbol{u}^s &= \widehat{\boldsymbol{\xi}} \boldsymbol{f}_p^I(\boldsymbol{q}, \boldsymbol{u}) &&= \widehat{\boldsymbol{\xi}} \dot{\boldsymbol{p}}^I \end{aligned} \tag{19}$$

Taking into account the last two equations, we arrive at

$$\dot{\boldsymbol{\psi}}_q^I \cdot \widehat{\boldsymbol{\xi}} \boldsymbol{q}_I + \dot{\boldsymbol{\psi}}_I^p \cdot \widehat{\boldsymbol{\xi}} \boldsymbol{p}^I + \boldsymbol{\psi}_q^I \cdot \widehat{\boldsymbol{\xi}} \dot{\boldsymbol{q}}_I + \boldsymbol{\psi}_I^p \cdot \widehat{\boldsymbol{\xi}} \dot{\boldsymbol{p}}^I = 0$$

The last equation is equivalent to

$$\frac{d}{dt} \left(\boldsymbol{\psi}_q^I \cdot \widehat{\boldsymbol{\xi}} \boldsymbol{q}_I + \boldsymbol{\psi}_I^p \cdot \widehat{\boldsymbol{\xi}} \boldsymbol{p}^I \right) = 0$$

or

$$\boldsymbol{\xi} \cdot \frac{d}{dt} \left(\boldsymbol{q}_I \times \boldsymbol{\psi}_q^I + \boldsymbol{p}^I \times \boldsymbol{\psi}_I^p \right) = 0$$

Accordingly, the generalized momentum map (65) is a conserved quantity of the optimal control problem.

Remark 1. If condition (15) holds for the special case $\boldsymbol{u}^s = \boldsymbol{u}$ (i.e. for any $s \in \mathbb{R}$), the mechanical control system has state-space symmetry in the sense of Grizzle & Marcus [16, 17]. Then symmetry condition (15) can be recast in the form

$$D\Phi_g(\boldsymbol{x}) \boldsymbol{f}(\boldsymbol{x}, \boldsymbol{u}) = \boldsymbol{f}(\Phi_g(\boldsymbol{x}), \boldsymbol{u}) \tag{20}$$

where the map $\Phi_g : \mathcal{P} \mapsto \mathcal{P}$ corresponds to the Lie group action of $g \in \mathrm{SO}(3)$ on $\boldsymbol{x} \in \mathcal{P}$. Using the nodal configuration and momentum vectors this map coincides with (12). If the system is uncontrolled, that is, if $\boldsymbol{u} = \boldsymbol{0}$, the state equations (2) can also be written in the form

$$\dot{\boldsymbol{x}} = X_{\mathcal{H}}(\boldsymbol{x})$$

If the underlying Hamiltonian system at hand has rotational symmetry, the Hamiltonian vector field $X_{\mathcal{H}}$ is $\mathrm{SO}(3)$-equivariant in the sense that

$$D\Phi_g(\boldsymbol{x}) X_{\mathcal{H}}(\boldsymbol{x}) = X_{\mathcal{H}}(\Phi_g(\boldsymbol{x})) \tag{21}$$

By comparing the last equation with (20), it is obvious that for mechanical control systems with state-space symmetry the symmetry of the uncontrolled system is a prerequisite for the symmetry of the mechanical control system. In general, the rotational symmetry of the underlying (uncontrolled) Hamiltonian system is passed on to the mechanical control system provided $\boldsymbol{u}^s$ exists such that symmetry condition (15) is satisfied.

3 STRUCTURE-PRESERVING DISCRETIZATION

We next devise a direct approach to the solution of the optimal control problem at hand that is capable to exactly conserve generalized momentum maps of the form (65) for mechanical optimal control systems with rotational symmetry. Our newly proposed approach accommodates a large class of one-step schemes for the integration of the state equations (1). To this end, the time interval of interest, $\mathcal{I} = [0, T]$, is devided into N non-overlapping sub-intervals whose length $h = t_{n+1} - t_n$ coincides with the time-step of the underlying one-step integrator.

Our approach relies on the introduction of a function $\mathbf{f_d} : \mathcal{P} \times \mathcal{P} \times \mathcal{U} \mapsto \mathbb{R}^{2n}$, which can be viewed as algorithmic approximation to the vector-valued function $h\boldsymbol{f} : \mathcal{P} \times \mathcal{U} \mapsto \mathbb{R}^{2n}$. Depending on the choice of $\mathbf{f_d}$ alternative one-step schemes of the form

$$\boldsymbol{x}_{n+1} - \boldsymbol{x}_n = \mathbf{f_d}(\boldsymbol{x}_n, \boldsymbol{x}_{n+1}, \boldsymbol{u}_n) \tag{22}$$

are generated. Similarly, the density cost function $L : \mathcal{P} \times \mathcal{U} \mapsto \mathbb{R}$ is approximated on each time interval by the expression $\mathrm{L_d}(\boldsymbol{x}_n, \boldsymbol{x}_{n+1}, \boldsymbol{u}_n)/h$. We refer to Section 4 for specific examples.

The newly proposed direct method is based on the introduction of the following discrete optimal control Lagrangian

$$\begin{aligned} J_d = &\boldsymbol{\psi}_0 \cdot (\boldsymbol{x}_0 - \overline{\boldsymbol{x}}_0) + \boldsymbol{\eta} \cdot \boldsymbol{g}_T(\boldsymbol{x}_N) + K(\boldsymbol{x}_N) \\ &+ \sum_{n=0}^{N-1} \left[\mathrm{L_d}(\boldsymbol{x}_n, \boldsymbol{a}_n, \boldsymbol{u}_n) + \boldsymbol{\psi}_{n+1} \cdot (\boldsymbol{x}_{n+1} - \boldsymbol{x}_n - \mathbf{f_d}(\boldsymbol{x}_n, \boldsymbol{a}_n, \boldsymbol{u}_n)) \right] \\ &+ \sum_{n=0}^{N-1} \left[\boldsymbol{\alpha}_n \cdot (\boldsymbol{a}_n - \boldsymbol{x}_n - \mathbf{f_d}(\boldsymbol{x}_n, \boldsymbol{a}_n, \boldsymbol{u}_n)) \right] \end{aligned} \tag{23}$$

The necessary optimality conditions are derived by imposing the stationary of (23). Accordingly, the following algebraic system of equations need be satisfied for arbitrary variations of $\boldsymbol{x}_n, \boldsymbol{\psi}_n$ ($n = 0, \dots, N$), $\boldsymbol{a}_n, \boldsymbol{u}_n, \boldsymbol{\alpha}_n$ ($n = 0, \dots, N-1$) and $\boldsymbol{\eta}$:

$$\sum_{n=0}^{N-1} \delta\boldsymbol{\psi}_{n+1} \cdot (\boldsymbol{x}_{n+1} - \boldsymbol{x}_n - \mathbf{f_d}(\boldsymbol{x}_n, \boldsymbol{a}_n, \boldsymbol{u}_n)) = 0 \tag{24a}$$

$$\sum_{n=0}^{N-1} \delta\boldsymbol{\alpha}_n \cdot (\boldsymbol{a}_n - \boldsymbol{x}_n - \mathbf{f_d}(\boldsymbol{x}_n, \boldsymbol{a}_n, \boldsymbol{u}_n)) = 0 \tag{24b}$$

$$\sum_{n=0}^{N-1} \delta\boldsymbol{x}_n \cdot \left(\boldsymbol{\psi}_{n+1} - \boldsymbol{\psi}_n + \boldsymbol{\alpha}_n - D_1\mathrm{L_d}(\boldsymbol{x}_n, \boldsymbol{a}_n, \boldsymbol{u}_n) + (\boldsymbol{\psi}_{n+1} + \boldsymbol{\alpha}_n) \cdot D_1\mathbf{f_d}(\boldsymbol{x}_n, \boldsymbol{a}_n, \boldsymbol{u}_n) \right) = 0 \tag{24c}$$

$$\sum_{n=0}^{N-1} \delta\boldsymbol{a}_n \cdot \left(\boldsymbol{\alpha}_n + D_2\mathrm{L_d}(\boldsymbol{x}_n, \boldsymbol{a}_n, \boldsymbol{u}_n) - (\boldsymbol{\psi}_{n+1} + \boldsymbol{\alpha}_n) \cdot D_2\mathbf{f_d}(\boldsymbol{x}_n, \boldsymbol{a}_n, \boldsymbol{u}_n) \right) = 0 \tag{24d}$$

$$\sum_{n=0}^{N-1} \delta\boldsymbol{u}_n \cdot \left(D_3\mathrm{L_d}(\boldsymbol{x}_n, \boldsymbol{a}_n, \boldsymbol{u}_n) - (\boldsymbol{\psi}_{n+1} + \boldsymbol{\alpha}_n) \cdot D_3\mathbf{f_d}(\boldsymbol{x}_n, \boldsymbol{a}_n, \boldsymbol{u}_n) \right) = 0 \tag{24e}$$

for $n = 0, \dots, N-1$ along with

$$\delta\boldsymbol{\psi}_0 \cdot (\boldsymbol{x}_0 - \overline{\boldsymbol{x}}_0) = 0 \tag{25a}$$

$$\delta\boldsymbol{\eta} \cdot \boldsymbol{g}_T(\boldsymbol{x}_N) = 0 \tag{25b}$$

$$\delta\boldsymbol{x}_N \cdot \left(\boldsymbol{\psi}_N + D\boldsymbol{g}_T(\boldsymbol{x}_N)^T\boldsymbol{\eta} + DK(\boldsymbol{x}_N) \right) = 0 \tag{25c}$$

Due to the independence of $\delta\boldsymbol{\psi}_{n+1}, \delta\boldsymbol{\alpha}_n$ ($n = 0, \dots, N-1$), equations (24a) and (24b) yield $\boldsymbol{a}_n = \boldsymbol{x}_{n+1}$ ($n = 0, \dots, N-1$) along with the discrete state equations (22). Altogether, the

present approach leads to the following system of algebraic equations:

$$\boldsymbol{x}_{n+1} - \boldsymbol{x}_n = \mathbf{f_d}(\boldsymbol{x}_n, \boldsymbol{x}_{n+1}, \boldsymbol{u}_n) \tag{26a}$$
$$\boldsymbol{\psi}_{n+1} - \boldsymbol{\psi}_n + \boldsymbol{\alpha}_n = D_1\mathrm{L_d}(\boldsymbol{x}_n, \boldsymbol{x}_{n+1}, \boldsymbol{u}_n) - (\boldsymbol{\psi}_{n+1} + \boldsymbol{\alpha}_n) \cdot D_1\mathbf{f_d}(\boldsymbol{x}_n, \boldsymbol{x}_{n+1}, \boldsymbol{u}_n) \tag{26b}$$
$$-\boldsymbol{\alpha}_n = D_2\mathrm{L_d}(\boldsymbol{x}_n, \boldsymbol{x}_{n+1}, \boldsymbol{u}_n) - (\boldsymbol{\psi}_{n+1} + \boldsymbol{\alpha}_n) \cdot D_2\mathbf{f_d}(\boldsymbol{x}_n, \boldsymbol{x}_{n+1}, \boldsymbol{u}_n) \tag{26c}$$
$$\mathbf{0} = D_3\mathrm{L_d}(\boldsymbol{x}_n, \boldsymbol{x}_{n+1}, \boldsymbol{u}_n) - (\boldsymbol{\psi}_{n+1} + \boldsymbol{\alpha}_n) \cdot D_3\mathbf{f_d}(\boldsymbol{x}_n, \boldsymbol{x}_{n+1}, \boldsymbol{u}_n) \tag{26d}$$

along with

$$\boldsymbol{x}_0 = \overline{\boldsymbol{x}}_0 \tag{27a}$$
$$\mathbf{0} = \boldsymbol{g}_T(\boldsymbol{x}_N) \tag{27b}$$
$$\boldsymbol{\psi}_N = -DK(\boldsymbol{x}_N) - D\boldsymbol{g}_T(\boldsymbol{x}_N)^T\boldsymbol{\eta} \tag{27c}$$

The above equations provide the general formulation of the necessary optimality conditions for the optimal control problem at hand. Specific schemes emanate from (26) by choosing appropriate expressions for $\mathbf{f_d}$ and $\mathrm{L_d}$. This will be further investigated in Section 4. First, however, we show that the general method (26) always generates schemes that are capable of conserving generalized momentum maps of the form (65).

3.1 Algorithmic conservation of the generalized momentum map

With regard to the partitioned form of the state equations, (5), the right-hand side of the discrete state equations introduced in (22) can be written in the form

$$\mathbf{f_d}(\boldsymbol{x}_n, \boldsymbol{x}_{n+1}, \boldsymbol{u}_n) = \begin{bmatrix} \mathbf{f_d}^q(\boldsymbol{p}_n, \boldsymbol{p}_{n+1}) \\ \mathbf{f_d}_p(\boldsymbol{q}_n, \boldsymbol{q}_{n+1}, \boldsymbol{u}_n) \end{bmatrix} \tag{28}$$

Similarly, the discrete version of the density cost function can be written as

$$\mathrm{L_d}(\boldsymbol{x}_n, \boldsymbol{x}_{n+1}, \boldsymbol{u}_n) = \mathrm{L_d}\left((\boldsymbol{q}_n, \boldsymbol{p}_n), (\boldsymbol{q}_{n+1}, \boldsymbol{p}_{n+1}), \boldsymbol{u}_n\right) \tag{29}$$

The partitioned form of the necessary optimality conditions (26) for the optimal control problem is given by

$$\boldsymbol{q}_{n+1} - \boldsymbol{q}_n = \mathbf{f_d}^q(\boldsymbol{p}_n, \boldsymbol{p}_{n+1}) \tag{30a}$$
$$\boldsymbol{p}_{n+1} - \boldsymbol{p}_n = \mathbf{f_d}_p(\boldsymbol{q}_n, \boldsymbol{q}_{n+1}, \boldsymbol{u}_n) \tag{30b}$$
$$\boldsymbol{\psi}_{q_{n+1}} - \boldsymbol{\psi}_{q_n} + \boldsymbol{\alpha}_{q_n} = \partial_{\boldsymbol{q}_n}\mathrm{L_d} - (\boldsymbol{\psi}^p_{n+1} + \boldsymbol{\alpha}^p_n) \cdot \partial_{\boldsymbol{q}_n}\mathbf{f_d}_p(\boldsymbol{q}_n, \boldsymbol{q}_{n+1}, \boldsymbol{u}_n) \tag{30c}$$
$$\boldsymbol{\psi}^p_{n+1} - \boldsymbol{\psi}^p_n + \boldsymbol{\alpha}^p_n = \partial_{\boldsymbol{p}_n}\mathrm{L_d} - (\boldsymbol{\psi}_{q_{n+1}} + \boldsymbol{\alpha}_{q_n}) \cdot \partial_{\boldsymbol{p}_n}\mathbf{f_d}^q(\boldsymbol{p}_n, \boldsymbol{p}_{n+1}) \tag{30d}$$
$$-\boldsymbol{\alpha}_{q_n} = \partial_{\boldsymbol{q}_{n+1}}\mathrm{L_d} - (\boldsymbol{\psi}^p_{n+1} + \boldsymbol{\alpha}^p_n) \cdot \partial_{\boldsymbol{q}_{n+1}}\mathbf{f_d}_p(\boldsymbol{q}_n, \boldsymbol{q}_{n+1}, \boldsymbol{u}_n) \tag{30e}$$
$$-\boldsymbol{\alpha}^p_n = \partial_{\boldsymbol{p}_{n+1}}\mathrm{L_d} - (\boldsymbol{\psi}_{q_{n+1}} + \boldsymbol{\alpha}_{q_n}) \cdot \partial_{\boldsymbol{p}_{n+1}}\mathbf{f_d}^q(\boldsymbol{p}_n, \boldsymbol{p}_{n+1}) \tag{30f}$$
$$\mathbf{0} = \partial_{\boldsymbol{u}_n}\mathrm{L_d} - (\boldsymbol{\psi}^p_{n+1} + \boldsymbol{\alpha}^p_n) \cdot \partial_{\boldsymbol{u}_n}\mathbf{f_d}_p(\boldsymbol{q}_n, \boldsymbol{q}_{n+1}, \boldsymbol{u}_n) \tag{30g}$$

for $n = 0, \ldots, N-1$. In the above equations $\mathrm{L_d}$ stands for $\mathrm{L_d}\left((\boldsymbol{q}_n, \boldsymbol{p}_n), (\boldsymbol{q}_{n+1}, \boldsymbol{p}_{n+1}), \boldsymbol{u}_n\right)$. Now assume that the optimal control problem under consideration has rotational symmetry. That is, conditions (15) and (16) are satisfied. Then viable discrete versions of the state equations and the density cost function will inherit these symmetry properties (see Section 4 for

specific examples). In particular, the following two conditions will be fulfilled on the discrete level:

$$\begin{aligned} \boldsymbol{R}^s \mathrm{f}_{\mathrm{d}I}^{\,q}(\boldsymbol{p}_n, \boldsymbol{p}_{n+1}) &= \mathrm{f}_{\mathrm{d}I}^{\,q}\left(\boldsymbol{R}^s \circ \boldsymbol{p}_n, \boldsymbol{R}^s \circ \boldsymbol{p}_{n+1}\right) \\ \boldsymbol{R}^s \mathrm{f}_{\mathrm{d}p}^{\,I}(\boldsymbol{q}_n, \boldsymbol{q}_{n+1}, \boldsymbol{u}_n) &= \mathrm{f}_{\mathrm{d}p}^{\,I}\left(\boldsymbol{R}^s \circ \boldsymbol{q}_n, \boldsymbol{R}^s \circ \boldsymbol{q}_{n+1}, \boldsymbol{u}_n^s\right) \end{aligned} \tag{31}$$

and

$$\mathrm{L_d}\left((\boldsymbol{R}^s \circ \boldsymbol{q}_n, \boldsymbol{R}^s \circ \boldsymbol{p}_n), (\boldsymbol{R}^s \circ \boldsymbol{q}_{n+1}, \boldsymbol{R}^s \circ \boldsymbol{p}_{n+1}), \boldsymbol{u}_n^s\right) = \mathrm{L_d}\left((\boldsymbol{q}_n, \boldsymbol{p}_n), (\boldsymbol{q}_{n+1}, \boldsymbol{p}_{n+1}), \boldsymbol{u}_n\right) \tag{32}$$

If these conditions hold the present method does conserve the generalized momentum map (65) in the sense that

$$J_\xi(\boldsymbol{q}_{n+1}, \boldsymbol{p}_{n+1}, \boldsymbol{\psi}_{q_{n+1}}, \boldsymbol{\psi}_{n+1}^p) = J_\xi(\boldsymbol{q}_n, \boldsymbol{p}_n, \boldsymbol{\psi}_{q_n}, \boldsymbol{\psi}_n^p) \tag{33}$$

for $n = 0, \ldots, N-1$. To prove this we start with the infinitesimal version of the discrete symmetry condition (32). Similar to (18) we calculate

$$\left.\frac{d}{ds}\right|_{s=0} \mathrm{L_d}\left((\boldsymbol{R}^s \circ \boldsymbol{q}_n, \boldsymbol{R}^s \circ \boldsymbol{p}_n), (\boldsymbol{R}^s \circ \boldsymbol{q}_{n+1}, \boldsymbol{R}^s \circ \boldsymbol{p}_{n+1}), \boldsymbol{u}_n^s\right) = 0$$

$$\partial_{\boldsymbol{q}_{I_n}} \mathrm{L_d} \cdot \widehat{\boldsymbol{\xi}} \boldsymbol{q}_{I_n} + \partial_{\boldsymbol{p}_n^I} \mathrm{L_d} \cdot \widehat{\boldsymbol{\xi}} \boldsymbol{p}_n^I + \partial_{\boldsymbol{q}_{I_{n+1}}} \mathrm{L_d} \cdot \widehat{\boldsymbol{\xi}} \boldsymbol{q}_{I_{n+1}} + \partial_{\boldsymbol{p}_{n+1}^I} \mathrm{L_d} \cdot \widehat{\boldsymbol{\xi}} \boldsymbol{p}_{n+1}^I + \partial_{\boldsymbol{u}_n} \mathrm{L_d} \cdot \left.\frac{d}{ds}\right|_{s=0} \boldsymbol{u}_n^s = 0$$

Inserting from (30c) through (30g) into the last equation yields

$$\begin{aligned} &\left[\boldsymbol{\psi}_{q_{n+1}}^I - \boldsymbol{\psi}_{q_n}^I + \boldsymbol{\alpha}_{q_n}^I + (\boldsymbol{\psi}_{n+1}^p + \boldsymbol{\alpha}_n^p) \cdot \partial_{\boldsymbol{q}_n} \mathrm{f}_{\mathrm{d}p}^{\,I}\right] \cdot \widehat{\boldsymbol{\xi}} \boldsymbol{q}_{I_n} \\ &+ \left[\boldsymbol{\psi}_{I_{n+1}}^p - \boldsymbol{\psi}_{I_n}^p + \boldsymbol{\alpha}_{I_n}^p + (\boldsymbol{\psi}_{q_{n+1}} + \boldsymbol{\alpha}_{q_n}) \cdot \partial_{\boldsymbol{p}_n} \mathrm{f}_{\mathrm{d}I}^{\,q}\right] \cdot \widehat{\boldsymbol{\xi}} \boldsymbol{p}_n^I \\ &+ \left[-\boldsymbol{\alpha}_{q_n}^I + (\boldsymbol{\psi}_{n+1}^p + \boldsymbol{\alpha}_n^p) \cdot \partial_{\boldsymbol{q}_{n+1}} \mathrm{f}_{\mathrm{d}p}^{\,I}\right] \cdot \widehat{\boldsymbol{\xi}} \boldsymbol{q}_{I_{n+1}} \\ &+ \left[-\boldsymbol{\alpha}_{I_n}^p + (\boldsymbol{\psi}_{q_{n+1}} + \boldsymbol{\alpha}_{q_n}) \cdot \partial_{\boldsymbol{p}_{n+1}} \mathrm{f}_{\mathrm{d}I}^{\,q}\right] \cdot \widehat{\boldsymbol{\xi}} \boldsymbol{p}_{n+1}^I \\ &+ \left(\boldsymbol{\psi}_{n+1}^p + \boldsymbol{\alpha}_n^p\right) \cdot \partial_{\boldsymbol{u}_n} \mathrm{f}_{\mathrm{d}p} \cdot \left.\frac{d}{ds}\right|_{s=0} \boldsymbol{u}_n^s = 0 \end{aligned} \tag{34}$$

On the other hand, the infinitesimal version of the discrete symmetry condition (31) can be derived in analogy to (19) and is given by

$$\begin{aligned} \partial_{\boldsymbol{p}_n^I} \mathrm{f}_{\mathrm{d}J}^{\,q} \cdot \widehat{\boldsymbol{\xi}} \boldsymbol{p}_n^I + \partial_{\boldsymbol{p}_{n+1}^I} \mathrm{f}_{\mathrm{d}J}^{\,q} \cdot \widehat{\boldsymbol{\xi}} \boldsymbol{p}_{n+1}^I &= \widehat{\boldsymbol{\xi}} \mathrm{f}_{\mathrm{d}J}^{\,q} = \widehat{\boldsymbol{\xi}}\left(\boldsymbol{q}_{J_{n+1}} - \boldsymbol{q}_{J_{n+1}}\right) \\ \partial_{\boldsymbol{q}_{I_n}} \mathrm{f}_{\mathrm{d}p}^{\,J} \cdot \widehat{\boldsymbol{\xi}} \boldsymbol{q}_{I_n} + \partial_{\boldsymbol{q}_{I_{n+1}}} \mathrm{f}_{\mathrm{d}p}^{\,J} \cdot \widehat{\boldsymbol{\xi}} \boldsymbol{q}_{I_{n+1}} + \partial_{\boldsymbol{u}_n} \mathrm{f}_{\mathrm{d}p}^{\,J} \cdot \left.\tfrac{d}{ds}\right|_{s=0} \boldsymbol{u}_n^s &= \widehat{\boldsymbol{\xi}} \mathrm{f}_{\mathrm{d}p}^{\,J} = \widehat{\boldsymbol{\xi}}\left(\boldsymbol{p}_{n+1}^J - \boldsymbol{p}_n^J\right) \end{aligned} \tag{35}$$

On the right-hand side of (35) the discrete state equations (30a) and (30b) have been taken into account. Substituting (35) into (34) yields

$$\boldsymbol{\psi}_{q_{n+1}}^I \cdot \widehat{\boldsymbol{\xi}} \boldsymbol{q}_{I_{n+1}} - \boldsymbol{\psi}_{q_n}^I \cdot \widehat{\boldsymbol{\xi}} \boldsymbol{q}_{I_n} + \boldsymbol{\psi}_{I_{n+1}}^p \cdot \widehat{\boldsymbol{\xi}} \boldsymbol{p}_{n+1}^I - \boldsymbol{\psi}_{I_n}^p \cdot \widehat{\boldsymbol{\xi}} \boldsymbol{p}_n^I = 0$$

or

$$\boldsymbol{\xi} \cdot \left(\boldsymbol{q}_{I_{n+1}} \times \boldsymbol{\psi}_{q_{n+1}}^I + \boldsymbol{p}_{n+1}^I \times \boldsymbol{\psi}_{I_{n+1}}^p - \boldsymbol{q}_{I_n} \times \boldsymbol{\psi}_{q_n}^I - \boldsymbol{p}_n^I \times \boldsymbol{\psi}_{I_n}^p\right) = 0$$

This result confirms algorithmic conservation of the generalized momentum map as stated in (33).

4 SPECIFIC SCHEMES

According to the direct approach to the solution of optimal control problems devised in the last section, the specific choice of one-step method for the integration of the state equations together with the specific discretization of the density cost function leads to a structure-preserving optimal control method that is capable of conserving the generalized momentum map. The purpose of this section is to further investigate and illustrate the design of specific schemes.

4.1 One-stage theta method

The discretization of the state equations by means of the one-stage theta method (see, for example, Stuart & Humphries [27]) relies on the specific choice

$$\mathbf{f_d}(\boldsymbol{x}_n, \boldsymbol{x}_{n+1}, \boldsymbol{u}_n) = h\boldsymbol{f}(\boldsymbol{x}_{n+\theta}, \boldsymbol{u}_n) \tag{36}$$

in the discrete state equations (22). Here,

$$\boldsymbol{x}_{n+\theta} = (1-\theta)\boldsymbol{x}_n + \theta\boldsymbol{x}_{n+1} \tag{37}$$

for $\theta \in [0,1]$. In the special case of uncontrolled Hamiltonian systems, the one-stage theta method comprises, for example, both forward ($\theta = 0$) and backward ($\theta = 1$) Euler methods and the implicit mid-point rule ($\theta = 1/2$). Similar to (36), for the discretization of the density cost function we choose $\mathrm{L_d}(\boldsymbol{x}_n, \boldsymbol{x}_{n+1}, \boldsymbol{u}_n) = hL(\boldsymbol{x}_{n+\theta}, \boldsymbol{u}_n)$. Before we substitute (36) into (26a) through (26d), we recast (26b) and (26c) in the form

$$\boldsymbol{\psi}_{n+1} - \boldsymbol{\psi}_n = D_1\mathrm{L_d} + D_2\mathrm{L_d} - (\boldsymbol{\psi}_{n+1} + \boldsymbol{\alpha}_n)\cdot(D_1\mathbf{f_d} + D_2\mathbf{f_d}) \tag{38a}$$

$$\boldsymbol{\psi}_{n+1} - \boldsymbol{\psi}_n + 2\boldsymbol{\alpha}_n = D_1\mathrm{L_d} - D_2\mathrm{L_d} - (\boldsymbol{\psi}_{n+1} + \boldsymbol{\alpha}_n)\cdot(D_1\mathbf{f_d} - D_2\mathbf{f_d}) \tag{38b}$$

With regard to (36) we have

$$\begin{aligned} D_1\mathbf{f_d}(\boldsymbol{x}_n, \boldsymbol{x}_{n+1}, \boldsymbol{u}_n) &= h(1-\theta)\partial_{\boldsymbol{x}}\boldsymbol{f}(\boldsymbol{x}_{n+\theta}, \boldsymbol{u}_n) \\ D_2\mathbf{f_d}(\boldsymbol{x}_n, \boldsymbol{x}_{n+1}, \boldsymbol{u}_n) &= h\theta\partial_{\boldsymbol{x}}\boldsymbol{f}(\boldsymbol{x}_{n+\theta}, \boldsymbol{u}_n) \end{aligned}$$

Similarly, we get

$$\begin{aligned} D_1\mathrm{L_d}(\boldsymbol{x}_n, \boldsymbol{x}_{n+1}, \boldsymbol{u}_n) &= h(1-\theta)\partial_{\boldsymbol{x}}L(\boldsymbol{x}_{n+\theta}, \boldsymbol{u}_n) \\ D_2\mathrm{L_d}(\boldsymbol{x}_n, \boldsymbol{x}_{n+1}, \boldsymbol{u}_n) &= h\theta\partial_{\boldsymbol{x}}L(\boldsymbol{x}_{n+\theta}, \boldsymbol{u}_n) \end{aligned}$$

Inserting these relationships into (38a) and (38b), a straightforward calculation yields

$$\boldsymbol{\alpha}_n = -\theta\left(\boldsymbol{\psi}_{n+1} - \boldsymbol{\psi}_n\right) \tag{39}$$

together with

$$\boldsymbol{\psi}_{n+1} - \boldsymbol{\psi}_n = h\partial_{\boldsymbol{x}}L(\boldsymbol{x}_{n+\theta}, \boldsymbol{u}_n) - h\boldsymbol{\psi}_{n+(1-\theta)}\cdot\partial_{\boldsymbol{x}}\boldsymbol{f}(\boldsymbol{x}_{n+\theta}, \boldsymbol{u}_n) \tag{40}$$

Eventually, (26d) yields the control equations

$$\mathbf{0} = \partial_{\boldsymbol{u}}L(\boldsymbol{x}_{n+\theta}, \boldsymbol{u}_n) - \boldsymbol{\psi}_{n+(1-\theta)}\cdot\partial_{\boldsymbol{u}}\boldsymbol{f}(\boldsymbol{x}_{n+\theta}, \boldsymbol{u}_n) \tag{41}$$

Note that (40) and (41) can be viewed as discrete counterparts of the adjoint equations (7b) and the control equations (7c), respectively. Box 1 contains a summary of the theta family of structure-preserving optimal control schemes just derived.

Remark 2. For $\theta =\in \{0, \frac{1}{2}\}$ the method summarized in Box 1 can be directly linked to the discrete maximum principle proposed by Guibout & Bloch [18] (see, respectively, *Störmer's rule* and the *midpoint scheme* in [18]).

Box 1: The structure-preserving theta method for optimal control.

Using the optimal control Hamiltonian (6), the structure-preserving theta method for optimal control can be written in the form

$$\begin{aligned}
\boldsymbol{x}_{n+1} - \boldsymbol{x}_n &= h\partial_{\boldsymbol{\psi}} H(\boldsymbol{x}_{n+\theta}, \boldsymbol{\psi}_{n+(1-\theta)}, \boldsymbol{u}_n) \\
\boldsymbol{\psi}_{n+1} - \boldsymbol{\psi}_n &= -h\partial_{\boldsymbol{x}} H(\boldsymbol{x}_{n+\theta}, \boldsymbol{\psi}_{n+(1-\theta)}, \boldsymbol{u}_n) \\
\boldsymbol{0} &= \partial_{\boldsymbol{u}} H(\boldsymbol{x}_{n+\theta}, \boldsymbol{\psi}_{n+(1-\theta)}, \boldsymbol{u}_n)
\end{aligned}$$

or

$$\begin{aligned}
\boldsymbol{x}_{n+1} - \boldsymbol{x}_n &= h\boldsymbol{f}(\boldsymbol{x}_{n+\theta}, \boldsymbol{u}_n) \\
\boldsymbol{\psi}_{n+1} - \boldsymbol{\psi}_n &= h\partial_{\boldsymbol{x}} L(\boldsymbol{x}_{n+\theta}, \boldsymbol{u}_n) - h\boldsymbol{\psi}_{n+(1-\theta)} \cdot \partial_{\boldsymbol{x}} \boldsymbol{f}(\boldsymbol{x}_{n+\theta}, \boldsymbol{u}_n) \\
\boldsymbol{0} &= \partial_{\boldsymbol{u}} L(\boldsymbol{x}_{n+\theta}, \boldsymbol{u}_n) - \boldsymbol{\psi}_{n+(1-\theta)} \cdot \partial_{\boldsymbol{u}} \boldsymbol{f}(\boldsymbol{x}_{n+\theta}, \boldsymbol{u}_n)
\end{aligned}$$

together with

$$\begin{aligned}
\boldsymbol{x}_0 &= \overline{\boldsymbol{x}}_0 \\
\boldsymbol{0} &= \boldsymbol{g}_T(\boldsymbol{x}_N) \\
\boldsymbol{\psi}_N &= -DK(\boldsymbol{x}_N) - D\boldsymbol{g}_T(\boldsymbol{x}_N)^T \boldsymbol{\eta}
\end{aligned}$$

4.2 Partitioned theta method

We next consider a variant of the one-stage theta method which takes into account the partitioned form of the state equations (5). In particular, we choose

$$\mathbf{f_d}(\boldsymbol{x}_n, \boldsymbol{x}_{n+1}, \boldsymbol{u}_n) = \begin{bmatrix} \mathbf{f_d}^q(\boldsymbol{p}_n, \boldsymbol{p}_{n+1}) \\ \mathbf{f_d}_p(\boldsymbol{q}_n, \boldsymbol{q}_{n+1}, \boldsymbol{u}_n) \end{bmatrix} = \begin{bmatrix} h\boldsymbol{f}^q(\boldsymbol{p}_{n+(1-\theta)}) \\ h\boldsymbol{f}_p(\boldsymbol{q}_{n+\theta}, \boldsymbol{u}_n) \end{bmatrix} \tag{42}$$

for $\theta \in [0,1]$. In the case of uncontrolled Hamiltonian systems the present choice embraces the symplectic Euler methods (cf. Hairer et al. [20]) which are obtained for $\theta = 0$ and $\theta = 1$, respectively. As before, the implicit mid-point rule is obtained for $\theta = 1/2$. Concerning the discrete version of the density cost function we further choose

$$\begin{aligned}
\mathrm{L_d}(\boldsymbol{x}_n, \boldsymbol{x}_{n+1}, \boldsymbol{u}_n) &= \mathrm{L_d}\left((\boldsymbol{q}_n, \boldsymbol{p}_n), (\boldsymbol{q}_{n+1}, \boldsymbol{p}_{n+1}), \boldsymbol{u}_n\right) \\
&= hL(\boldsymbol{q}_{n+\theta}, \boldsymbol{p}_{n+(1-\theta)}, \boldsymbol{u}_n)
\end{aligned} \tag{43}$$

In analogy to the last section we start with (38) to derive the resulting optimal control scheme. For completeness, we consider a more general version of (42) which is also valid for non-separable Hamiltonians. Accordingly, instead of (38) we consider

$$\mathbf{f_d}(\boldsymbol{x}_n, \boldsymbol{x}_{n+1}, \boldsymbol{u}_n) = \begin{bmatrix} h\boldsymbol{f}^q(\boldsymbol{q}_{n+\theta}, \boldsymbol{p}_{n+(1-\theta)}) \\ h\boldsymbol{f}_p(\boldsymbol{q}_{n+\theta}, \boldsymbol{p}_{n+(1-\theta)}, \boldsymbol{u}_n) \end{bmatrix} \tag{44}$$

Performing the derivatives needed in (38), we obtain

$$\begin{aligned}
D_1\mathbf{f_d}(\boldsymbol{x}_n, \boldsymbol{x}_{n+1}, \boldsymbol{u}_n) &= h \begin{bmatrix} (1-\theta)\partial_{\boldsymbol{q}} \boldsymbol{f}^q(\boldsymbol{q}_{n+\theta}, \boldsymbol{p}_{n+(1-\theta)}) & \theta\partial_{\boldsymbol{p}} \boldsymbol{f}^q(\boldsymbol{q}_{n+\theta}, \boldsymbol{p}_{n+(1-\theta)}) \\ (1-\theta)\partial_{\boldsymbol{q}} \boldsymbol{f}_p(\boldsymbol{q}_{n+\theta}, \boldsymbol{p}_{n+(1-\theta)}, \boldsymbol{u}_n) & \theta\partial_{\boldsymbol{p}} \boldsymbol{f}_p(\boldsymbol{q}_{n+\theta}, \boldsymbol{p}_{n+(1-\theta)}, \boldsymbol{u}_n) \end{bmatrix} \\
D_2\mathbf{f_d}(\boldsymbol{x}_n, \boldsymbol{x}_{n+1}, \boldsymbol{u}_n) &= h \begin{bmatrix} \theta\partial_{\boldsymbol{q}} \boldsymbol{f}^q(\boldsymbol{q}_{n+\theta}, \boldsymbol{p}_{n+(1-\theta)}) & (1-\theta)\partial_{\boldsymbol{p}} \boldsymbol{f}^q(\boldsymbol{q}_{n+\theta}, \boldsymbol{p}_{n+(1-\theta)}) \\ \theta\partial_{\boldsymbol{q}} \boldsymbol{f}_p(\boldsymbol{q}_{n+\theta}, \boldsymbol{p}_{n+(1-\theta)}, \boldsymbol{u}_n) & (1-\theta)\partial_{\boldsymbol{p}} \boldsymbol{f}_p(\boldsymbol{q}_{n+\theta}, \boldsymbol{p}_{n+(1-\theta)}, \boldsymbol{u}_n) \end{bmatrix}
\end{aligned}$$

Furthermore,

$$D_1\mathrm{L_d}(\boldsymbol{x}_n,\boldsymbol{x}_{n+1},\boldsymbol{u}_n) = h\begin{bmatrix}(1-\theta)\partial_{\boldsymbol{q}}L(\boldsymbol{q}_{n+\theta},\boldsymbol{p}_{n+(1-\theta)},\boldsymbol{u}_n)\\ \theta\partial_{\boldsymbol{p}}L(\boldsymbol{q}_{n+\theta},\boldsymbol{p}_{n+(1-\theta)},\boldsymbol{u}_n)\end{bmatrix}$$
$$D_2\mathrm{L_d}(\boldsymbol{x}_n,\boldsymbol{x}_{n+1},\boldsymbol{u}_n) = h\begin{bmatrix}\theta\partial_{\boldsymbol{q}}L(\boldsymbol{q}_{n+\theta},\boldsymbol{p}_{n+(1-\theta)},\boldsymbol{u}_n)\\ \theta(1-\theta)\partial_{\boldsymbol{p}}L(\boldsymbol{q}_{n+\theta},\boldsymbol{p}_{n+(1-\theta)},\boldsymbol{u}_n)\end{bmatrix}$$

Now, inserting these relationships into (38a) and (38b), a straightforward calculation along the lines of the last section yields

$$\begin{aligned}\boldsymbol{\alpha}_{q_n} =& -\theta\left(\boldsymbol{\psi}_{q_{n+1}}-\boldsymbol{\psi}_{q_n}\right)\\ \boldsymbol{\alpha}_n^p =&(\theta-1)\left(\boldsymbol{\psi}_{n+1}^p-\boldsymbol{\psi}_n^p\right)\end{aligned} \tag{45}$$

along with

$$\begin{aligned}\begin{bmatrix}\boldsymbol{\psi}_{q_{n+1}}-\boldsymbol{\psi}_{q_n}\\ \boldsymbol{\psi}_{n+1}^p-\boldsymbol{\psi}_n^p\end{bmatrix} =& h\begin{bmatrix}\partial_{\boldsymbol{q}}L(\boldsymbol{q}_{n+\theta},\boldsymbol{p}_{n+(1-\theta)},\boldsymbol{u}_n)\\ \partial_{\boldsymbol{p}}L(\boldsymbol{q}_{n+\theta},\boldsymbol{p}_{n+(1-\theta)},\boldsymbol{u}_n)\end{bmatrix}\\ &-h\begin{bmatrix}\partial_{\boldsymbol{q}}\boldsymbol{f}^{q^T}(\boldsymbol{q}_{n+\theta},\boldsymbol{p}_{n+(1-\theta)}) & \partial_{\boldsymbol{q}}f_p^T(\boldsymbol{q}_{n+\theta},\boldsymbol{p}_{n+(1-\theta)},\boldsymbol{u}_n)\\ \partial_{\boldsymbol{p}}\boldsymbol{f}^{q^T}(\boldsymbol{q}_{n+\theta},\boldsymbol{p}_{n+(1-\theta)}) & \partial_{\boldsymbol{p}}f_p^T(\boldsymbol{q}_{n+\theta},\boldsymbol{p}_{n+(1-\theta)},\boldsymbol{u}_n)\end{bmatrix}\begin{bmatrix}\boldsymbol{\psi}_{q_{n+(1-\theta)}}\\ \boldsymbol{\psi}_{n+\theta}^p\end{bmatrix}\end{aligned} \tag{46}$$

Eventually, (26d) yields the control equations

$$\boldsymbol{0} = \partial_{\boldsymbol{u}}L(\boldsymbol{q}_{n+\theta},\boldsymbol{p}_{n+(1-\theta)},\boldsymbol{u}_n) - \partial_{\boldsymbol{u}}f_p^T(\boldsymbol{q}_{n+\theta},\boldsymbol{p}_{n+(1-\theta)},\boldsymbol{u}_n)\boldsymbol{\psi}_{n+\theta}^p \tag{47}$$

To summarize, the newly derived structure-preserving partitioned theta method for optimal control problems consists of the discrete state equations resulting from (44) (or (42) for separable Hamiltonians associated with the mechanical control system), the discrete adjoint equations (46) and the discrete control equations (47). A compact form of this scheme is given in terms of the optimal control Hamiltonian and can be found in Box 2. Note that the special case of a separable Hamiltonian associated with the underlying mechanical control system results if the optimal control Hamiltonian (11) is used in Box 2.

Remark 3. For $\theta = 1$ the method summarized in Box 2 coincides with the symplectic discrete-time state-adjoint system developed by Flaßkamp & Murphey [13] in the context of a linear optimal control problem (LQR).

4.3 Energy-momentum schemes

In the forward dynamics of Hamiltonian systems energy-momentum (EM) integrators preserve both the total mechanical energy and momentum maps associated with symmetries of the mechanical system. EM schemes (and energy-dissipative variants thereof, see, for example Armero & Romero [2]) can also be used for the discretization of the underlying Hamiltonian system related to the mechanical control systems under consideration. For this purpose we now choose in the discrete state equations (22)

$$\mathbf{f_d}(\boldsymbol{x}_n,\boldsymbol{x}_{n+1},\boldsymbol{u}_n) = \begin{bmatrix}\mathbf{f_d}^q(\boldsymbol{p}_n,\boldsymbol{p}_{n+1})\\ \mathbf{f_d}_p(\boldsymbol{q}_n,\boldsymbol{q}_{n+1},\boldsymbol{u}_n)\end{bmatrix} = \begin{bmatrix}h\boldsymbol{M}^{-1}\boldsymbol{p}_{n+\frac{1}{2}}\\ -h\overline{\nabla}\mathcal{V}(\boldsymbol{q}_n,\boldsymbol{q}_{n+1}) + h\boldsymbol{B}(\boldsymbol{q}_{n+\frac{1}{2}})\boldsymbol{u}_n\end{bmatrix} \tag{48}$$

Here, $\overline{\nabla}\mathcal{V}(\boldsymbol{q}_n,\boldsymbol{q}_{n+1})$ denotes a discrete derivative of the potential function $\mathcal{V}$ in the sense of Gonzalez [15]. The control extension of EM schemes yields energy-momentum consistent

Box 2: The structure-preserving partitioned theta method for optimal control.

$$
\begin{aligned}
\boldsymbol{q}_{n+1} - \boldsymbol{q}_n &= h\partial_{\boldsymbol{\psi}_q} H(\boldsymbol{q}_{n+\theta}, \boldsymbol{p}_{n+(1-\theta)}, \boldsymbol{\psi}_{q_{n+(1-\theta)}}, \boldsymbol{\psi}^p_{n+\theta}, \boldsymbol{u}_n) \\
\boldsymbol{p}_{n+1} - \boldsymbol{p}_n &= h\partial_{\boldsymbol{\psi}^p} H(\boldsymbol{q}_{n+\theta}, \boldsymbol{p}_{n+(1-\theta)}, \boldsymbol{\psi}_{q_{n+(1-\theta)}}, \boldsymbol{\psi}^p_{n+\theta}, \boldsymbol{u}_n) \\
\boldsymbol{\psi}_{q_{n+1}} - \boldsymbol{\psi}_{q_n} &= -h\partial_{\boldsymbol{q}} H(\boldsymbol{q}_{n+\theta}, \boldsymbol{p}_{n+(1-\theta)}, \boldsymbol{\psi}_{q_{n+(1-\theta)}}, \boldsymbol{\psi}^p_{n+\theta}, \boldsymbol{u}_n) \\
\boldsymbol{\psi}^p_{n+1} - \boldsymbol{\psi}^p_n &= -h\partial_{\boldsymbol{p}} H(\boldsymbol{q}_{n+\theta}, \boldsymbol{p}_{n+(1-\theta)}, \boldsymbol{\psi}_{q_{n+(1-\theta)}}, \boldsymbol{\psi}^p_{n+\theta}, \boldsymbol{u}_n) \\
\boldsymbol{0} &= \partial_{\boldsymbol{u}} H(\boldsymbol{q}_{n+\theta}, \boldsymbol{p}_{n+(1-\theta)}, \boldsymbol{\psi}_{q_{n+(1-\theta)}}, \boldsymbol{\psi}^p_{n+\theta}, \boldsymbol{u}_n)
\end{aligned}
$$

together with

$$
\begin{aligned}
\boldsymbol{q}_0 &= \overline{\boldsymbol{q}}_0 \\
\boldsymbol{p}_0 &= \overline{\boldsymbol{p}}_0 \\
\boldsymbol{0} &= \boldsymbol{g}_T(\boldsymbol{q}_N, \boldsymbol{p}_N) \\
\boldsymbol{\psi}_{q_N} &= -\partial_{\boldsymbol{q}} K(\boldsymbol{q}_N, \boldsymbol{p}_N) - \boldsymbol{\eta} \cdot \partial_{\boldsymbol{q}} \boldsymbol{g}_T(\boldsymbol{q}_N, \boldsymbol{p}_N) \\
\boldsymbol{\psi}^p_N &= -\partial_{\boldsymbol{p}} K(\boldsymbol{q}_N, \boldsymbol{p}_N) - \boldsymbol{\eta} \cdot \partial_{\boldsymbol{p}} \boldsymbol{g}_T(\boldsymbol{q}_N, \boldsymbol{p}_N)
\end{aligned}
$$

schemes which are capable of exactly reproducing the balance laws for energy and angular momentum in the discrete setting. We refer to Betsch & Sänger for further investigations in this direction. Concerning the discrete version of the density cost function we choose

$$
\mathrm{L_d}(\boldsymbol{x}_n, \boldsymbol{x}_{n+1}, \boldsymbol{u}_n) = hL(\boldsymbol{x}_{n+\frac{1}{2}}, \boldsymbol{u}_n) \tag{49}
$$

which corresponds to the choice $\theta = \frac{1}{2}$ in the last two sections. Again, inserting (48) and (49) into (26) yields a direct method for the optimal control problem which is capable of conserving the generalized momentum map (65). We refer to Section 5 for a sample application of an EM scheme.

4.4 Structure-preservation on two levels

This section provides a summary of the structure-preserving properties of the numerical methods dealt with in this paper. First of all we recall the specific form of the affine Hamiltonian control systems under consideration. With regard to (5) the state equations can be written in the form

$$
\begin{aligned}
\dot{\boldsymbol{q}}_I &= \boldsymbol{f}^q_I(\boldsymbol{p}) &&= (M^{-1})_{IJ}\boldsymbol{p}^J \\
\dot{\boldsymbol{p}}^I &= \boldsymbol{f}^I_p(\boldsymbol{q}, \boldsymbol{u}) &&= -\partial_{\boldsymbol{q}_I}\mathcal{V}(\boldsymbol{q}) + \boldsymbol{f}^I_{\mathrm{ext}}(\boldsymbol{q}, \boldsymbol{u})
\end{aligned} \tag{50}
$$

Note that the underlying Hamiltonian system is given by

$$
\begin{aligned}
\dot{\boldsymbol{q}}_I &= (M^{-1})_{IJ}\boldsymbol{p}^J \\
\dot{\boldsymbol{p}}^I &= -\partial_{\boldsymbol{q}_I}\mathcal{V}(\boldsymbol{q})
\end{aligned} \tag{51}
$$

Suppose that the underlying Hamiltonian system has rotational symmetry. This implies that the potential energy function is invariant under superposed rotations. That is, using the notation introduced in Section 2.2,

$$
\mathcal{V}(\boldsymbol{R}^s \circ \boldsymbol{q}) = \mathcal{V}(\boldsymbol{q}) \tag{52}
$$

Performing the time derivative of (52) yields

$$\begin{aligned} \tfrac{d}{dt}\mathcal{V}(\boldsymbol{R}^s \circ \boldsymbol{q}) &= \tfrac{d}{dt}\mathcal{V}(\boldsymbol{q}) \\ \partial_{\boldsymbol{q}_I}\mathcal{V}(\boldsymbol{R}^s \circ \boldsymbol{q}) \cdot \boldsymbol{R}^s \dot{\boldsymbol{q}}_I &= \partial_{\boldsymbol{q}_I}\mathcal{V}(\boldsymbol{q}) \cdot \boldsymbol{R}^s \dot{\boldsymbol{q}}_I \end{aligned}$$

A straightforward calculation leads to the result

$$\big(\boldsymbol{R}^s \partial_{\boldsymbol{q}_I}\mathcal{V}(\boldsymbol{q}) - \partial_{\boldsymbol{q}_I}\mathcal{V}(\boldsymbol{R}^s \circ \boldsymbol{q})\big) \cdot \boldsymbol{R}^s \dot{\boldsymbol{q}}_I = 0$$

which has to hold for arbitrary nodal velocities $\dot{\boldsymbol{q}}_I$. Due to the non-singularity of the rotation matrix $\boldsymbol{R}^s$, the last equation implies

$$\boldsymbol{R}^s \partial_{\boldsymbol{q}_I}\mathcal{V}(\boldsymbol{q}) = \partial_{\boldsymbol{q}_I}\mathcal{V}(\boldsymbol{R}^s \circ \boldsymbol{q}) \tag{53}$$

Moreover, in view of $(50)_1$ and $(51)_1$, we get

$$\boldsymbol{f}_I^q(\boldsymbol{R}^s \circ \boldsymbol{p}) = (M^{-1})_{IJ}\boldsymbol{R}^s \boldsymbol{p}^J = \boldsymbol{R}^s \boldsymbol{f}_I^q(\boldsymbol{p}) \tag{54}$$

Note that (54) and (53) corroborate $\mathrm{SO}(3)$-equivariance of the Hamiltonian vector field as stated in (21) (see Remark 1). We further calculate the infinitesimal version of invariance property (52):

$$\left.\frac{d}{ds}\right|_{s=0} \mathcal{V}(\boldsymbol{R}^s \circ \boldsymbol{q}) = \partial_{\boldsymbol{q}_I}\mathcal{V}(\boldsymbol{q}) \cdot \widehat{\boldsymbol{\xi}}\boldsymbol{q}_I = 0$$

The last equation can be recast in the form

$$\boldsymbol{\xi} \cdot \big(\boldsymbol{q}_I \times \partial_{\boldsymbol{q}_I}\mathcal{V}(\boldsymbol{q})\big) = 0 \tag{55}$$

We remark that a similar calculation based on (53) yields the same result.

4.4.1 Mechanical control system

It is well-known that a mechanical control system satisfies fundamental mechanical balance laws. In the present work we focus on the balance laws for angular momentum and energy, respectively. A time-stepping scheme for the numerical integration of the state equations shall be called structure-preserving mechanical integrator[1] if these balance laws are exactly reproduced. Correspondingly, the specific integrator applied to the mechanical control system can be associated with the first level of structure preservation. The angular momentum of a mechanical system relative to the origin of an inertial frame is defined by

$$\boldsymbol{j} = \boldsymbol{q}_I \times \boldsymbol{p}^I \tag{56}$$

It can be verified by a straightforward calculation that the following relationship holds:

$$\boldsymbol{j}_{n+1} - \boldsymbol{j}_n = \boldsymbol{q}_{I_{n+\theta}} \times \big(\boldsymbol{p}^I_{n+1} - \boldsymbol{p}^I_n\big) - \boldsymbol{p}^I_{n+(1-\theta)} \times \big(\boldsymbol{q}_{I_{n+1}} - \boldsymbol{q}_{I_n}\big)$$

for $\theta \in [0,1]$. If we now apply the partitioned theta method (see (42) in Section 4.2), the last equation yields

$$\boldsymbol{j}_{n+1} - \boldsymbol{j}_n = h\boldsymbol{q}_{I_{n+\theta}} \times \partial_{\boldsymbol{q}_I}\mathcal{V}(\boldsymbol{q}_{n+\theta}) - h(M^{-1})_{IJ}\boldsymbol{p}^I_{n+(1-\theta)} \times \boldsymbol{p}^J_{n+(1-\theta)} + h\boldsymbol{q}_{I_{n+\theta}} \times \boldsymbol{f}^I(\boldsymbol{q}_{n+\theta}, \boldsymbol{u}_n)$$

[1]The term mechanical integrator has originally been coined by Marsden [24] in the context of conservative mechanical systems with symmetry.

Taking into account the symmetry properties (55) and $(M^{-1})_{IJ} = (M^{-1})_{JI}$, the last equation leads to the result

$$\boldsymbol{\xi} \cdot \left(\boldsymbol{j}_{n+1} - \boldsymbol{j}_n \right) = h \boldsymbol{\xi} \cdot \left(\boldsymbol{q}_{I_{n+\theta}} \times \boldsymbol{f}^I(\boldsymbol{q}_{n+\theta}, \boldsymbol{u}_n) \right) \tag{57}$$

Accordingly, all members of the theta method are capable of conserving angular momentum in the case of vanishing controls (i.e. $\boldsymbol{f}^I = \boldsymbol{0}$). Moreover, for mechanical control systems the balance law for angular momentum will be consistently reproduced according to the discrete balance law (57). Analogous conclusions can be drawn in the case of the energy-momentum scheme outlined in Section 4.3. Moreover, concerning the theta method dealt with in Section 4.1, the only angular momentum consistent method is the implicit mid-point rule ($\theta = \frac{1}{2}$). Note that a time-stepping scheme that is not capable to conserve angular momentum in the purely Hamiltonian case will in general fail to correctly reproduce balance of angular momentum for finite time steps.

Of the one-step schemes considered herein, the energy-momentum integrator is the only energy consistent method. Taking into account the properties of the discrete derivative in (48), it can be verified that, similar to (57), the discrete balance law for the energy is satisfied for arbitrary time steps according to

$$\mathcal{H}(\boldsymbol{q}_{n+1}, \boldsymbol{p}_{n+1}) - \mathcal{H}(\boldsymbol{q}_n, \boldsymbol{p}_n) = \left(\boldsymbol{q}_{I_{n+1}} - \boldsymbol{q}_{I_n} \right) \cdot \boldsymbol{f}^I(\boldsymbol{q}_{n+\frac{1}{2}}, \boldsymbol{u}_n) \tag{58}$$

Here, the Hamiltonian $\mathcal{H}(\boldsymbol{q}_{n+1}, \boldsymbol{p}_{n+1})$ has been defined in (3) and corresponds to the total mechanical energy of the system. Note that in the case of vanishing controls, i.e. if $\boldsymbol{f}^I = \boldsymbol{0}$, the energy-momentum integrator conserves the total energy.

4.4.2 Optimal control problem

The second level of structure preservation is associated with the optimal control problem. Indeed, as has been proven in Section 3.1, by design the present approach yields numerical methods capable of conserving generalized momentum maps related to rotational symmetries of the optimal control problem. This 2nd level conservation property holds, irrespective of the one-step scheme used for the integration of the state equations. That is, the two levels of structure preservation turn out to be independent of each other.

Since the optimal control problem itself has an intrinsic Hamiltonian structure, the optimal control Hamiltonian defined in (6) is also a conserved quantity. Note however, that the numerical methods developed in this work are not capable of conserving the Hamiltonian of the optimal control problem for a finite number of time steps. This issue will be further investigated in the context of the numerical example presented in Section 5.

5 NUMERICAL EXAMPLE

5.1 Nonlinear spring pendulum

The numerical example deals with the nonlinear spring pendulum depicted in Fig. 1. The motion of the controlled mechanical system at hand is governed by state equations of the form (5). In particular, we have

$$\begin{aligned} \dot{\boldsymbol{q}} &= \boldsymbol{M}^{-1} \boldsymbol{p} \\ \dot{\boldsymbol{p}} &= -D\mathcal{V}(\boldsymbol{q}) + \boldsymbol{B}(\boldsymbol{q}) \boldsymbol{u} \end{aligned}$$

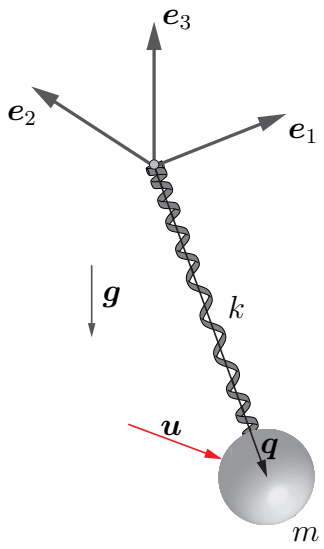

Figure 1: The nonlinear spring pendulum

Here, $\boldsymbol{q} \in \mathbb{R}^3$ is the position vector of the particle with mass m. Relative to the inertial Cartesian basis $\{\boldsymbol{e}_i\}$ (see Fig.1) we have $\boldsymbol{q}(t) = q_i(t)\boldsymbol{e}_i$. The mass matrix is diagonal and given by $\boldsymbol{M} = m\boldsymbol{I}$. The potential energy function assumes the form

$$\mathcal{V}(\boldsymbol{q}) = \underbrace{-\boldsymbol{g}\cdot\boldsymbol{M}\boldsymbol{q}}_{=\mathcal{V}_{\text{ext}}(\boldsymbol{q})} + \underbrace{\frac{1}{2}kl_0^2\varepsilon(\boldsymbol{q})^2}_{=\mathcal{V}_{\text{int}}(\boldsymbol{q})} \tag{59}$$

where

$$\boldsymbol{g} = -g\boldsymbol{e}_3 \tag{60}$$

is the gravitational acceleration and

$$\varepsilon(\boldsymbol{q}) = \frac{1}{2\,l_0^2}\left(\boldsymbol{q}\cdot\boldsymbol{q} - l_0^2\right) \tag{61}$$

is a scalar Green-Lagrangian-type strain measure. Note that the potential energy can be split into an external part $\mathcal{V}_{\text{ext}}$ due to gravity and an internal part $\mathcal{V}_{\text{int}}$ due to deformation of the spring. In (61), $l_0 = \sqrt{\boldsymbol{q}_0\cdot\boldsymbol{q}_0}$ defines the strain-free state of the spring. The motion of the spring pendulum is controlled by a force acting on particle m. That is, in the state equations $\boldsymbol{B}(\boldsymbol{q}) = \boldsymbol{I}$ such that the actuating force coincides with $\boldsymbol{u} \in \mathbb{R}^3$.

5.1.1 Symmetry properties

It can be easily verified that the potential energy is invariant under superposed rotations about the $\boldsymbol{e}_3$-axis. That is, setting $\boldsymbol{R}_3^s = \exp(s\widehat{\boldsymbol{e}}_3)$ and taking into account the identity $\boldsymbol{R}_3^s\boldsymbol{e}_3 = \boldsymbol{e}_3$, it can be deduced from (59) that

$$\mathcal{V}(\boldsymbol{R}_3^s\boldsymbol{q}) = \mathcal{V}(\boldsymbol{q}) \tag{62}$$

The last equation corresponds to symmetry property (52). Consequently, corresponding to (53), the identity

$$\boldsymbol{R}_3^s D\mathcal{V}(\boldsymbol{q}) = D\mathcal{V}(\boldsymbol{R}_3^s\boldsymbol{q})$$

holds. It can now be easily checked that symmetry condition (15) is satisfied provided that

$$\boldsymbol{u}^s = \boldsymbol{R}_3^s \boldsymbol{u} \tag{63}$$

Accordingly, the present mechanical control system has rotational symmetry about the $\boldsymbol{e}_3$-axis. Moreover, we choose the density cost function

$$\mathrm{L}(\boldsymbol{u}) = \frac{1}{2}\boldsymbol{u} \cdot \boldsymbol{u} \tag{64}$$

such that $\mathrm{L}(\boldsymbol{u}^s) = \mathrm{L}(\boldsymbol{u})$ and symmetry condition (16) is also satisfied. Accordingly, the optimal control problem under consideration has rotational symmetry about the $\boldsymbol{e}_3$-axis. Consequently, the associated generalized momentum map

$$J_3 = \boldsymbol{e}_3 \cdot \left(\boldsymbol{q} \times \boldsymbol{\psi}_q + \boldsymbol{p} \times \boldsymbol{\psi}^p \right) \tag{65}$$

is a conserved quantity.

5.1.2 Specific schemes under investigation

Of the newly developed structure-preserving schemes dealt with in Section 4 we apply the theta method (Section 4.1) with $\theta \in \{0, \frac{1}{2}, 1\}$, the partitioned theta method (Section 4.2) with $\theta \in \{0, \frac{1}{2}, 1\}$, and the energy-momentum scheme outlined in Section 4.3. Note that both the theta method and the partitioned theta method rely on

$$\begin{aligned} \mathbf{f}_{\mathrm{d}p}(\boldsymbol{q}_n, \boldsymbol{q}_{n+1}, \boldsymbol{u}_n) &= -hD\mathcal{V}(\boldsymbol{q}_{n+\theta}) + h\boldsymbol{u}_n \\ &= -hmg\boldsymbol{e}_3 - hk\varepsilon(\boldsymbol{q}_{n+\theta})\boldsymbol{q}_{n+\theta} + h\boldsymbol{u}_n \end{aligned} \tag{66}$$

in the discrete state equations. In contrast to that, the energy-momentum integrator is based on

$$\begin{aligned} \mathbf{f}_{\mathrm{d}p}(\boldsymbol{q}_n, \boldsymbol{q}_{n+1}, \boldsymbol{u}_n) &= -h\overline{\nabla}\mathcal{V}(\boldsymbol{q}_n, \boldsymbol{q}_{n+1}) + h\boldsymbol{u}_n \\ &= -hmg\boldsymbol{e}_3 - \frac{hk}{2}\left(\varepsilon(\boldsymbol{q}_n) + \varepsilon(\boldsymbol{q}_{n+1})\right)\boldsymbol{q}_{n+\frac{1}{2}} + h\boldsymbol{u}_n \end{aligned} \tag{67}$$

where use has been made of the discrete derivative of the internal potential function given by

$$\overline{\nabla}\mathcal{V}_{\mathrm{int}}(\boldsymbol{q}_n, \boldsymbol{q}_{n+1}) = \frac{k}{2}\left(\varepsilon(\boldsymbol{q}_n) + \varepsilon(\boldsymbol{q}_{n+1})\right)\boldsymbol{q}_{n+\frac{1}{2}} \tag{68}$$

The methods under investigation are summarized in Table 1. Note that the schemes **theta-$\frac{1}{2}$** and **ptheta-$\frac{1}{2}$** coincide.

5.1.3 Numerical results

In the optimal control problem under investigation both the initial and the terminal state of the spring pendulum are prescribed. The goal is to determine the maneuver of the spring pendulum between the prescribed start and end points such that the control effort is minimized. The data used in the numerical example is summarized in Table 2.

First of all, the converged numerical solution obtained with a high resolution of $N = 10000$ time steps is depicted in Figs. 2, 3 and 4. In particular, Fig. 2 contains the time evolution of the state coordinates $\boldsymbol{q}(t) = q_i(t)\boldsymbol{e}^i$, $\boldsymbol{p}(t) = p^i(t)\boldsymbol{e}_i$ and the associated adjoint variables

denomination	method
theta-0	theta method
theta-$\frac{1}{2}$	(Section 4.1)
theta-1	$\theta \in \{0, \frac{1}{2}, 1\}$
ptheta-0	partitioned theta method
ptheta-$\frac{1}{2}$	(Section 4.2)
ptheta-1	$\theta \in \{0, \frac{1}{2}, 1\}$
EM	energy-momentum method
	(Section 4.3)

Table 1: Nonlinear spring pendulum: Methods under investigation

m (mass)	1
k (spring constant)	0.6
g (gravity)	9.8
l_0	5
$\overline{\boldsymbol{q}}_0$ (initial)	$(-2, -5, -5)$
$\overline{\boldsymbol{p}}_0$	$(-3, 0, 0)$
$\overline{\boldsymbol{q}}_N$ (terminal)	$(2, -10, -4)$
$\overline{\boldsymbol{p}}_N$	$(0, 0, 0)$
T	5
$\varepsilon_{\text{Newton}}$	10^{-9}

Table 2: Nonlinear spring pendulum: Data used in the numerical example

$\boldsymbol{\psi}_q(t) = \psi_q^i(t)\boldsymbol{e}_i$, $\boldsymbol{\psi}^p(t) = \psi_i^p(t)\boldsymbol{e}^i$. Fig. 3 depicts the controls $\boldsymbol{u} = u^i\boldsymbol{e}_i$ and Fig. 4 shows the evolution of mechanical energies and angular momentum.

In Fig. 5 the fulfillment of the balance law for the mechanical energy is checked for a comparatively rough resolution of $N = 50$ time steps. Specifically, formula (58) for the discrete balance of energy is applied to the present problem and yields

$$\mathcal{R}_{n+1}^{\text{En}} = \mathcal{H}(\boldsymbol{q}_{n+1}, \boldsymbol{p}_{n+1}) - \mathcal{H}(\boldsymbol{q}_n, \boldsymbol{p}_n) - \big(\boldsymbol{q}_{n+1} - \boldsymbol{q}_n\big) \cdot \boldsymbol{u}_n \tag{69}$$

As expected, the only energy consistent method which exactly satisfies the discrete balance of energy in the sense that $\mathcal{R}_{n+1} = 0$ (up to numerical round-off errors) for $n = 0, \ldots, N-1$ is the scheme **EM**. Of course, for $N \to \infty$ (or $h \to 0$), $\mathcal{R}_{n+1} \to 0$ for all schemes under consideration.

The discrete fulfillment of the balance law for angular momentum can be checked by adapting (57) to the present problem. Accordingly, in Fig. 6 we consider the residual

$$\mathcal{R}_{n+1}^{\text{AM}} = \boldsymbol{e}_3 \cdot \Big(\boldsymbol{j}_{n+1} - \boldsymbol{j}_n - h\boldsymbol{q}_{I_{n+\theta}} \times \boldsymbol{u}_n\Big) \tag{70}$$

for $n = 0, \ldots, N-1$. Note that for the scheme **EM**, $\theta = \frac{1}{2}$ has to be used in (70). It can be observed from Fig. 6 that the schemes **ptheta-0**, **theta-$\frac{1}{2}$**, **ptheta-1** and **EM** are indeed

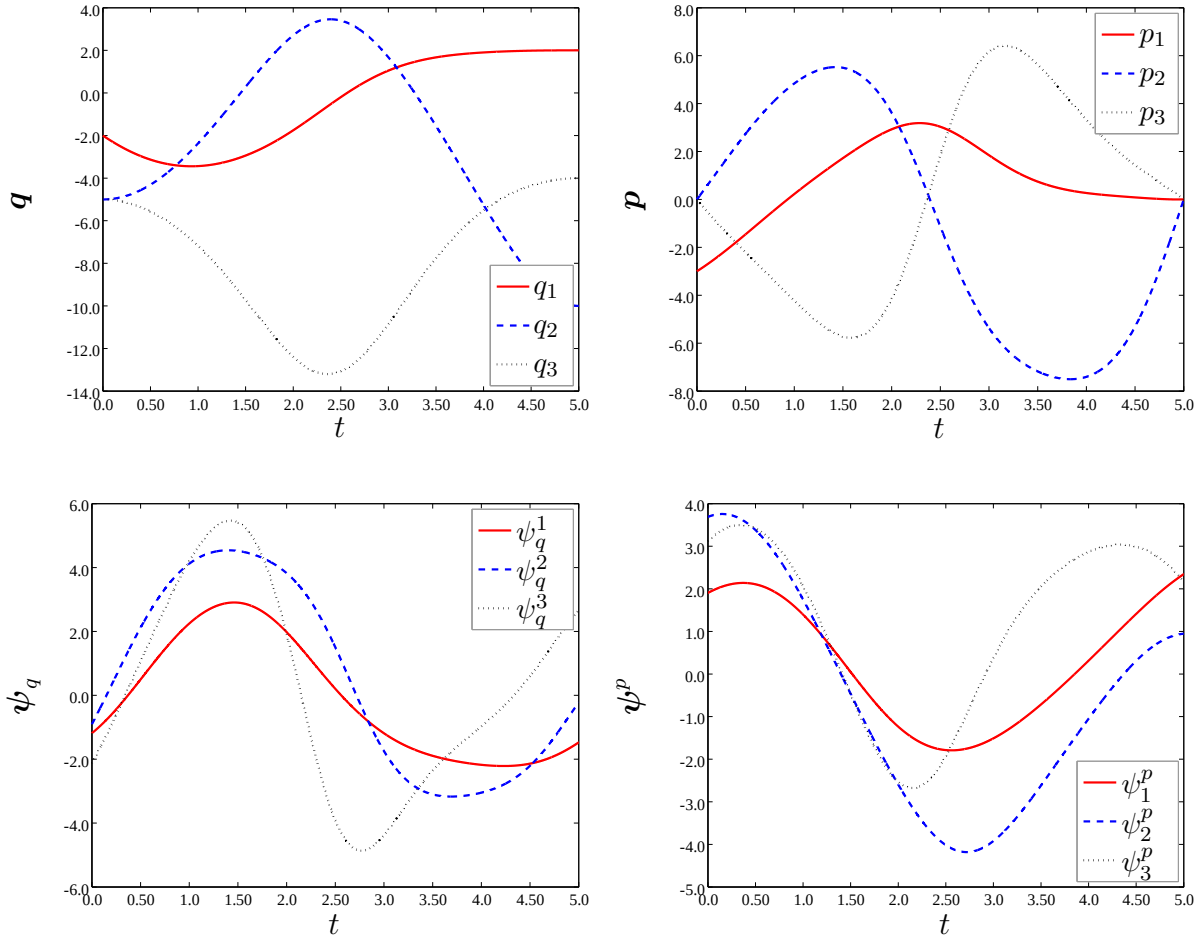

Figure 2: Nonlinear spring pendulum: State coordinates $(\boldsymbol{q}, \boldsymbol{p})$ and adjoint coordinates $(\boldsymbol{\psi}_q, \boldsymbol{\psi}^p)$ obtained with a high resolution of $N = 10000$ time steps

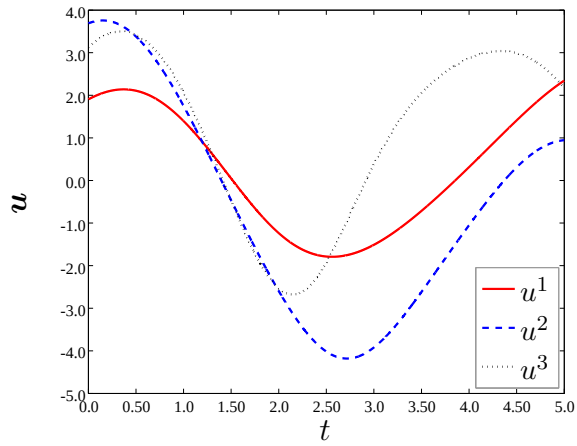

Figure 3: Nonlinear spring pendulum: Controls $\boldsymbol{u}$ obtained with a high resolution of $N = 10000$ time steps

consistently reproducing balance of angular momentum up to numerical round-off errors. This is in sharp contrast to the schemes **theta-0** and **theta-1**. Again this type of consistency error decreases when number N is increased.

Next the structure-preserving properties related to the second level (cf. Section 4.4.2) are

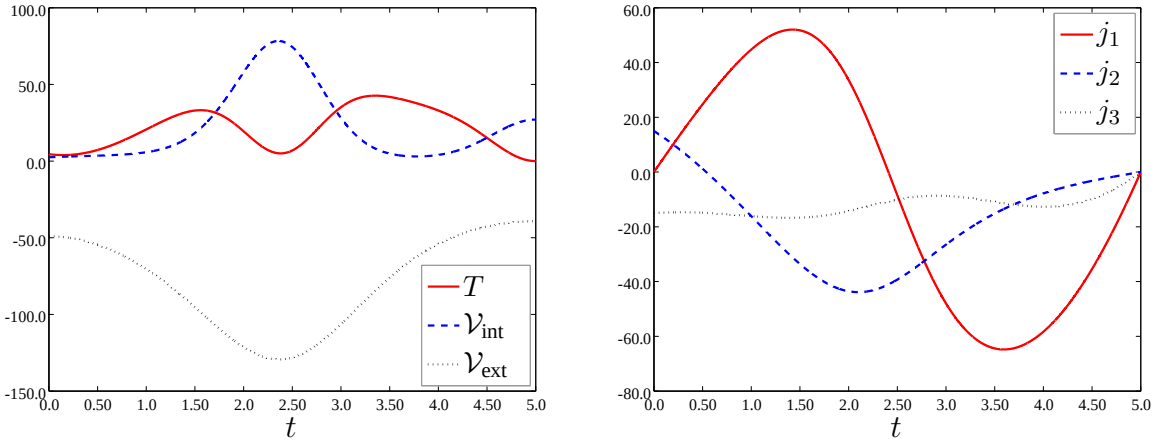

Figure 4: Nonlinear spring pendulum: Kinetic energy $T = \frac{1}{2}\boldsymbol{p} \cdot \boldsymbol{M}^{-1}\boldsymbol{p}$, gravitational potential energy $\mathcal{V}_{\text{ext}}$, strain energy $\mathcal{V}_{\text{int}}$ of the nonlinear spring and components $j_i = \boldsymbol{e}_i \cdot (\boldsymbol{q} \times \boldsymbol{p})$ of angular momentum obtained with a high resolution of $N = 10000$ time steps

considered. By design all schemes under investigation exactly preserve the generalized momentum map (65) associated with the rotational symmetry of the present optimal control problem. For completeness this conservation property is corroborated by Fig. 7 for the schemes **ptheta-0**, **theta-$\frac{1}{2}$**, **ptheta-1** and **EM**. Similarly, this conservation property holds (again up to numerical round-off errors) for the remaining schemes **theta-0** and **theta-1**.

As has been mentioned in Section 4.4.2, the optimal control Hamiltonian is also a 2nd level conserved quantity. However, as expected, none of the schemes under investigation exactly reproduces this conservation property. This can be observed from Figs. 8 through 10. The reference value of the constant optimal control Hamiltonian is equal to -0.37. All of the schemes under investigation converge to this reference value. However, for low resolutions of the optimal control problem significant deviations from the reference value can be observed (Figs. 8 through 10).

The errors in the state variables $\boldsymbol{x}$ and the adjoint variables $\boldsymbol{\psi}$ have been calculated via

$$\begin{aligned} \varepsilon_x &= \frac{1}{N+1}\sum_{n=0}^{N}\frac{||\boldsymbol{x}(t_n) - \boldsymbol{x}_{\text{ref}}(t_n)||_2}{||\boldsymbol{x}_{\text{ref}}||_2} \\ \varepsilon_\psi &= \frac{1}{N+1}\sum_{n=0}^{N}\frac{||\boldsymbol{\psi}(t_n) - \boldsymbol{\psi}_{\text{ref}}(t_n)||_2}{||\boldsymbol{\psi}_{\text{ref}}||_2} \end{aligned} \tag{71}$$

The corresponding plots are depicted in Figs. 11 and 12. It can be seen that the schemes **theta-$\frac{1}{2}$** and **EM** are second-order accurate whereas the schemes **theta-0**, **theta-1**, **ptheta-0** and **ptheta-1** are first-order accurate.

Eventually, to illustrate the calculated optimal solution, Fig. 13 shows a sequence of snapshots at successive points in time. In addition to the trajectory of particle m, the arrows indicate both magnitude (corresponding to the lengths of the arrows) and direction of the control force acting on particle m.

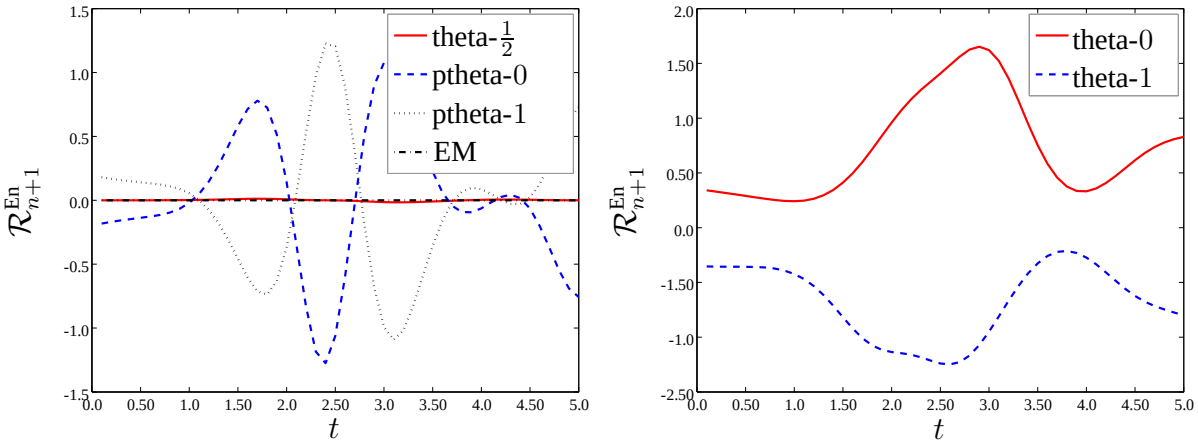

Figure 5: Nonlinear spring pendulum: Balance of energy for a low resolution of $N = 50$ time steps. The non-fulfillment of the balance of energy is measured by the residual $\mathcal{R}^{\mathrm{En}}_{n+1}$ defined in (69)

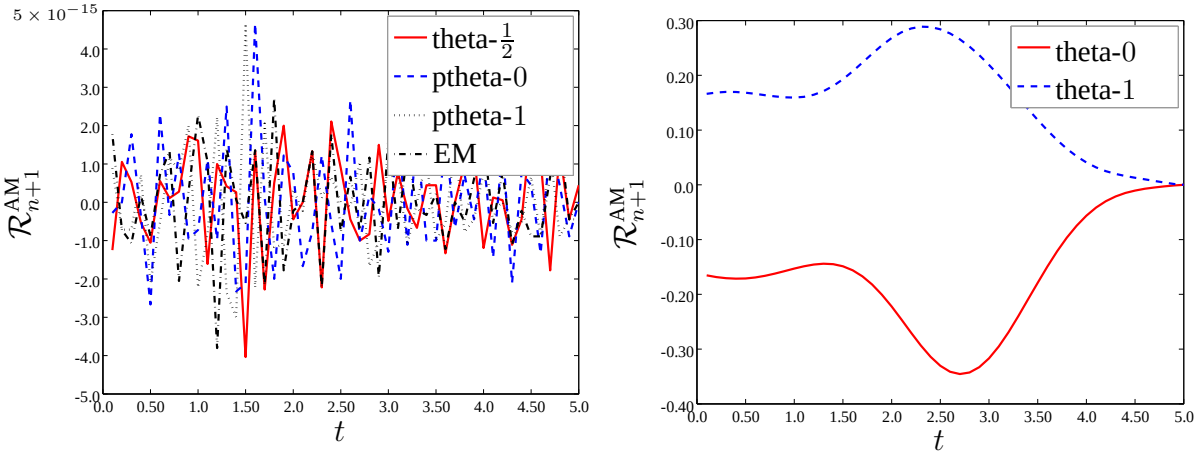

Figure 6: Nonlinear spring pendulum: Balance of angular momentum for a low resolution of $N = 50$ time steps. The non-fulfillment of the balance of angular momentum is measured by the residual $\mathcal{R}^{\mathrm{AM}}_{n+1}$ defined in (70)

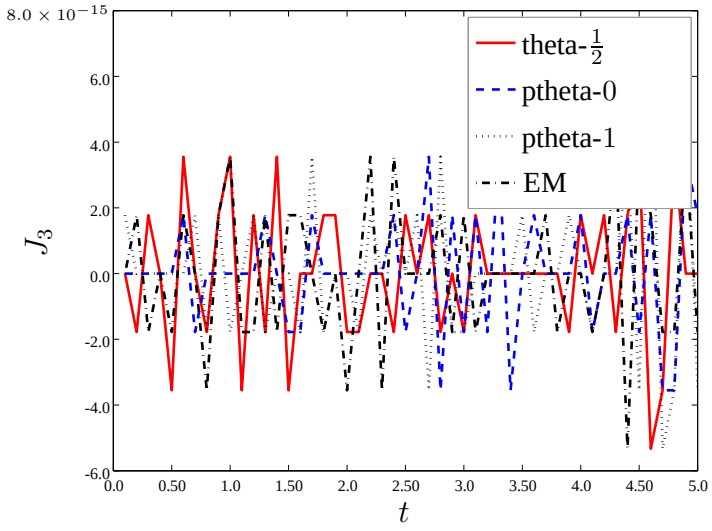

Figure 7: Nonlinear spring pendulum: Algorithmic conservation of the generalized momentum map J_3, cf. (65), up to numerical round-off errors. The optimal control problem has been solved with a low resolution of $N = 50$ time steps

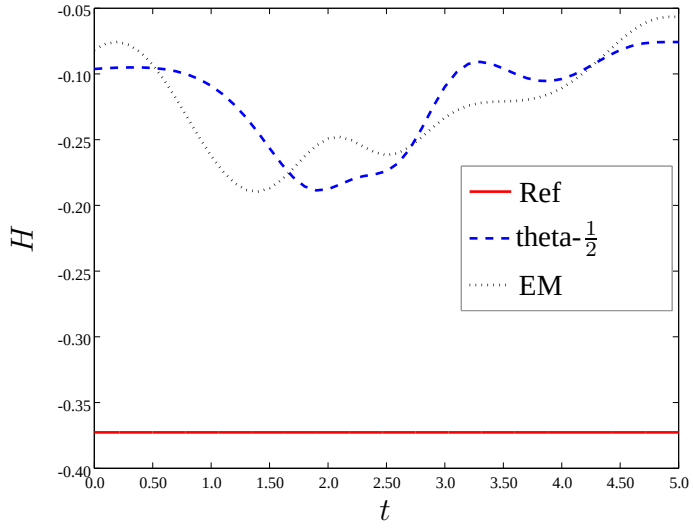

Figure 8: Nonlinear spring pendulum: Optimal control Hamiltonian obtained with the schemes **theta-$\frac{1}{2}$** and **EM** for $N = 50$ time steps. The (constant) reference value equals -0.37

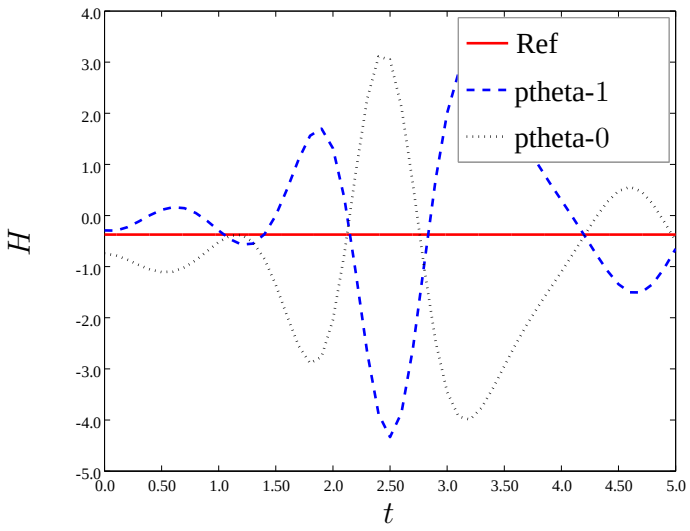

Figure 9: Nonlinear spring pendulum: Optimal control Hamiltonian obtained with the schemes **ptheta-0** and **ptheta-1** for $N = 50$ time steps. The (constant) reference value equals -0.37

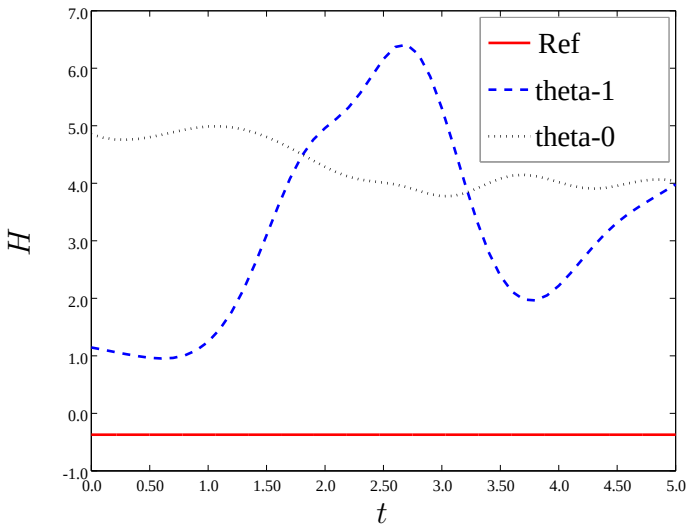

Figure 10: Nonlinear spring pendulum: Optimal control Hamiltonian obtained with the schemes **theta-0** and **theta-1** for $N = 50$ time steps. The (constant) reference value equals -0.37

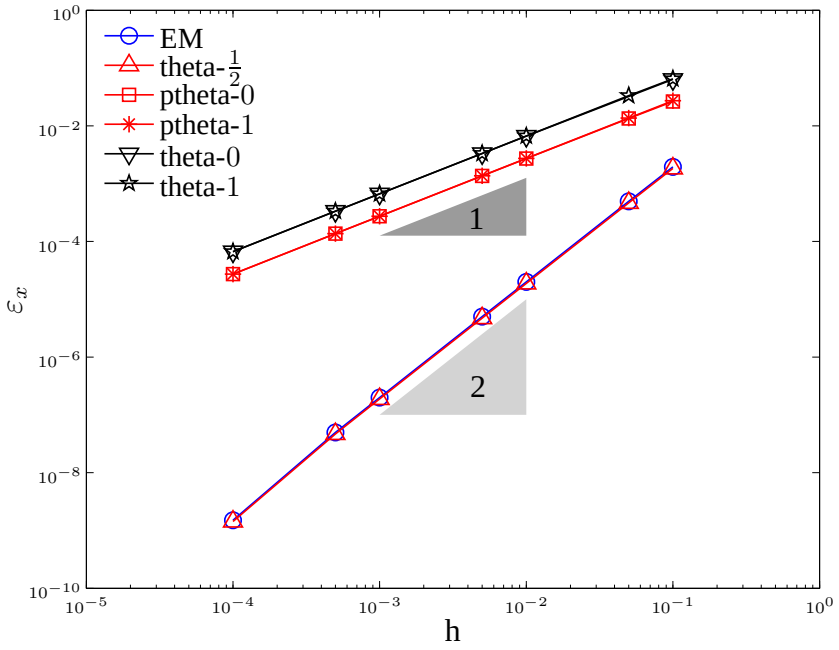

Figure 11: Nonlinear spring pendulum: Error ε_x in the state variables

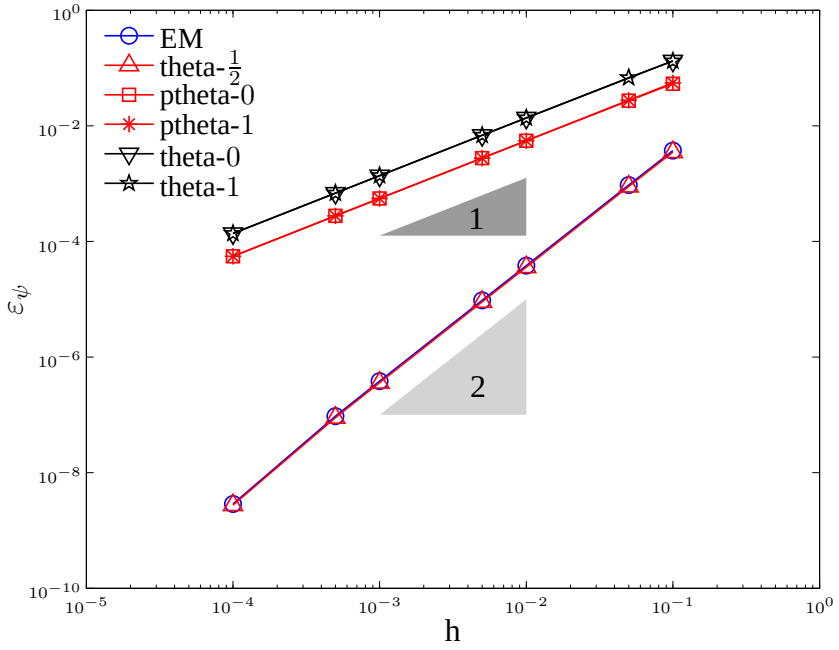

Figure 12: Nonlinear spring pendulum: Error ε_ψ in the adjoint variables

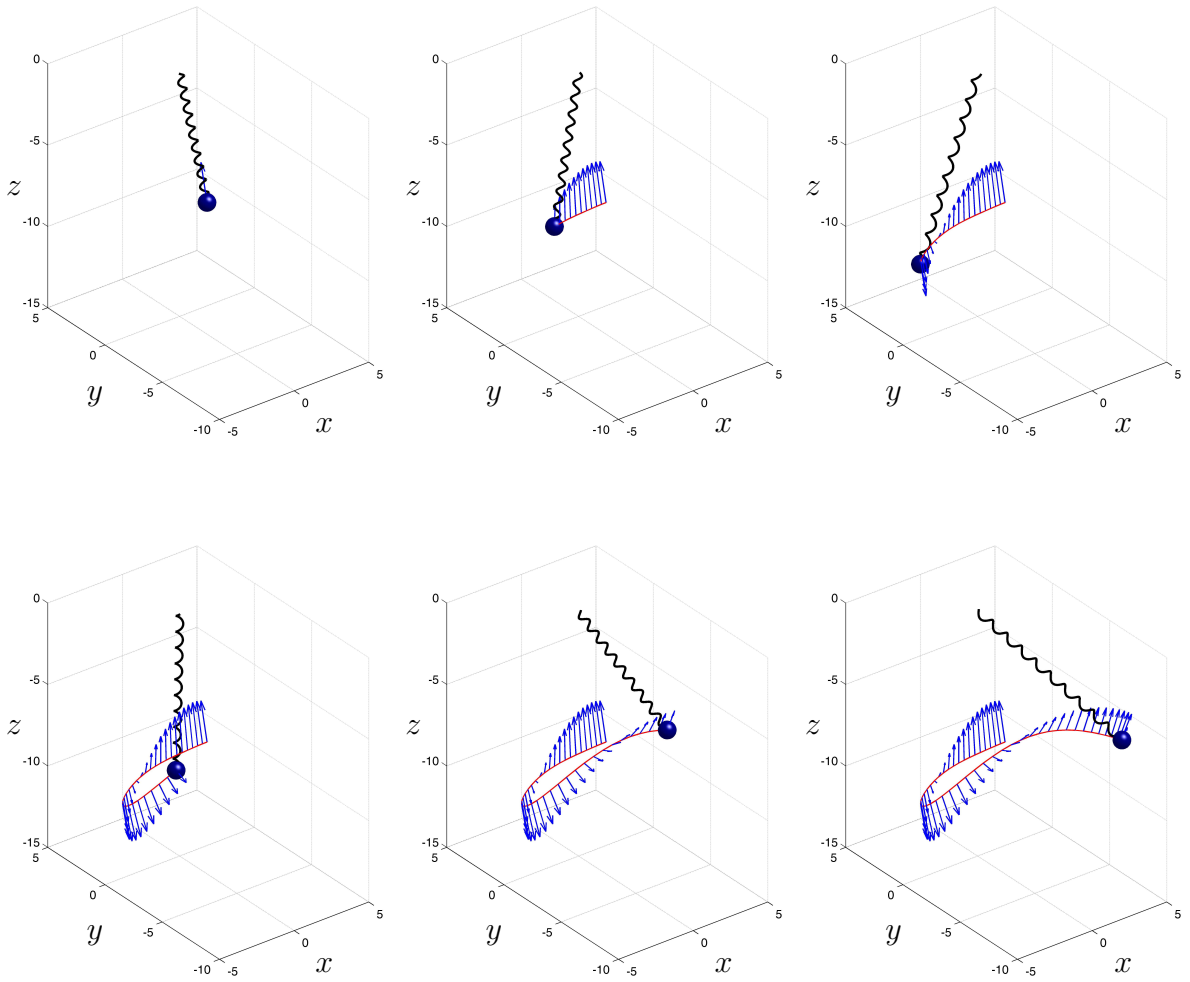

Figure 13: Nonlinear spring pendulum: Snapshots of the motion at times $t \in \{0, 1, 2, 3, 4, 5\}$

6 CONCLUSIONS

We devised a new structure-preserving direct approach to the numerical solution of optimal control problems in the framework of finite-dimensional mechanical systems. We may distinguish between two levels of structure-preservation. The first level of structure-preservation is linked to the forward dynamics of the underlying mechanical control system. That is, structure-preserving integrators such as momentum-symplectic or energy-momentum schemes can be applied to the numerical integration of the state equations. The second level of structure-preservation is connected to the optimal control problem itself. We saw that under specific symmetry conditions generalized momentum maps are conserved along an optimal path.

The newly devised direct method for the solution of the optimal control problem in Section 3 generates a family of schemes that by design conserve generalized momentum maps associated with rotational symmetries of the optimal control problem. To some extend our approach is related to previous work of Hager [19], Ober-Blöbaum et al. [26], Flaßkamp & Murphey [13] and Campos et al. [10]. Although those works do not consider symmetries and associated generalized momentum maps, the design of the discrete optimal control Lagrangian (23) hinges heavily on the *State Uniqueness Property* of the discrete control problem considered in Hager [19, Sec. 2].

Acknowledgement

Support for this research was provided by the Deutsche Forschungsgemeinschaft (DFG) under Grant BE 2285/10-1. This support is gratefully acknowledged.

REFERENCES

[1] S.K. Agrawal and B.C. Fabien. *Optimization of Dynamic Systems*. Kluwer Academic Publishers, 1999.

[2] F. Armero and I. Romero. On the formulation of high-frequency dissipative time-stepping algorithms for nonlinear dynamics. Part II: Second-order methods. *Comput. Methods Appl. Mech. Engrg.*, 190:6783–6824, 2001.

[3] P. Betsch, R. Siebert, and N. Sänger. Natural coordinates in the optimal control of multibody systems. *J. Comput. Nonlinear Dynam.*, 7(1):011009/1–8, 2012.

[4] J.T. Betts. *Practical Methods for Optimal Control and Estimation Using Nonlinear Programming*. SIAM, Philadelphia, PA, 2nd edition, 2010.

[5] L.T. Biegler. *Nonlinear Programming. Concepts, Algorithms, and Applications to Chemical Processes*. SIAM, Philadelphia, 2010.

[6] T. Binder, L. Blank, H.G. Bock, R. Bulirsch, W. Dahmen, M. Diehl, T. Kronseder, W. Marquardt, J.P. Schlöder, and O. von Stryk. Introduction to model based optimization of chemical processes on moving horizons. In M. Grötschel, S.O. Krumke, and J. Rambau, editors, *Online Optimization of Large Scale Systems*, pages 295–340. Springer-Verlag, 2001.

[7] A.M. Bloch. *Nonholonomic Mechanics and Control*. Springer-Verlag, 2003.

[8] A.M. Bloch, I.I. Hussein, M. Leok, and A.K. Sanyal. Geometric structure-preserving optimal control of a rigid body. *Journal of Dynamical and Control Systems*, 15(3):307–330, 2009.

[9] C.L. Bottasso and A. Croce. Optimal control of multibody systems using an energy preserving direct transcription method. *Multibody System Dynamics*, 12(1):17–45, 2004.

[10] C.M. Campos, S. Ober-Blöbaum, and E. Trlélat. High order variational integrators in the optimal control of mechanical systems. *Discrete and Continuous Dynamical Systems – Series A (DCDS-A)*, 35(9):4193–4223, 2015.

[11] M. Diehl, H.G. Bock, H. Diedam, and P.-B. Wieber. Fast direct multiple shooting algorithms for optimal robot control. In M. Diehl and K. Mombaur, editors, *Fast Motions in Biomechanics and Robotics*, volume 340 of *Lecture Notes in Control and Information Sciences*, pages 65–93. Springer-Verlag, 2006.

[12] D.S. Djukić. Noether's theorem for optimum control systems. *Int. J. Control*, 18(3):667–672, 1973.

[13] K. Flaßkamp and T.D. Murphey. Structure-preserving integration for linear optimal control and filtering of mechanical systems. Preprint March 2015.

[14] M. Gerdts. *Optimal Control of ODEs and DAEs*. De Gruyter, Berlin/Boston, 2012.

[15] O. Gonzalez. Time integration and discrete Hamiltonian systems. *J. Nonlinear Sci.*, 6:449–467, 1996.

[16] J. Grizzle and S. Marcus. Optimal control of systems possessing symmetries. *IEEE Transactions on Automatic Control*, 29(11):1037–1040, 1984.

[17] J. Grizzle and S. Marcus. The structure of nonlinear control systems possessing symmetries. *IEEE Transactions on Automatic Control*, 30(3):248–258, 1985.

[18] V. Guibout and A.M. Bloch. A discrete maximum principle for solving optimal control problems. In *Proceedings of the 43rd IEEE Conference on Decision and Control*, pages 1806–1811, Atlantis, Paradise Island, Bahamas, 2004.

[19] W.W. Hager. Runge-Kutta methods in optimal control and the transformed adjoint system. *Numer. Math.*, 87(2):247–282, 2000.

[20] E. Hairer, C. Lubich, and G. Wanner. *Geometric Numerical Integration*. Springer-Verlag, 2nd edition, 2006.

[21] M.W. Koch and S. Leyendecker. Energy momentum consistent force formulation for the optimal control of multibody systems. *Multibody System Dynamics*, 29:381–401, 2013.

[22] S. Leyendecker, S. Ober-Blöbaum, J.E. Marsden, and M. Ortiz. Discrete mechanics and optimal control for constrained systems. *Optim. Control Appl. Meth.*, 31(6):505–528, 2010.

[23] G. Little and E.R. Pinch. The Pontryagin maximum principle: the constancy of the Hamiltonian. *IMA J Math Control Info*, 13(4):403–408, 1996.

[24] J.E. Marsden. *Lectures on Mechanics*. Cambridge University Press, 1992.

[25] J.E. Marsden and T.S. Ratiu. *Introduction to Mechanics and Symmetry*. Springer-Verlag, 2nd edition, 1999.

[26] S. Ober-Blöbaum, O. Junge, and J.E. Marsden. Discrete mechanics and optimal control: An analysis. *ESAIM: Control, Optimisation and Calculus of Variations*, 17(2):322–352, 2011.

[27] A.M. Stuart and A.R. Humphries. *Dynamical Systems and Numerical Analysis*. Cambridge University Press, 1996.

[28] D.F.M. Torres. Conservation laws in optimal control. In F. Colonius and L. Grüne, editors, *Dynamics, Bifurcations, and Control*, volume 273 of *Lecture Notes in Control and Information Sciences*, pages 287–296. Springer-Verlag, 2002.

[29] D.F.M. Torres. On the Noether theorem for optimal control. *European Journal of Control*, 8(1):56–63, 2002.

[30] A.J. van der Schaft. Symmetries in optimal control. *SIAM J. Control and Optimization*, 25(2):245–259, 1987.